the plant journal

SEB SOCIETY FOR EXPERIMENTAL BIOLOGY

The Plant Journal (2024) doi: 10.1111/tpj.16626

The peptide GOLVEN10 alters root development and noduletaxis in *Medicago truncatula*

Sonali Roy[1,2], Ivone Torres-Jerez[2,3], Shulan Zhang[2,3], Wei Liu[2], Katharina Schiessl[4], Divya Jain[1], Clarissa Boschiero[2], Hee-Kyung Lee[3], Nicholas Krom[2], Patrick X. Zhao[2], Jeremy D. Murray[5], Giles E. D. Oldroyd[4], Wolf-Rüdiger Scheible[2] and Michael Udvardi[2,6,*]

[1]*College of Agriculture, Tennessee State University, Nashville, Tennessee 37209, USA,*
[2]*Noble Research Institute, LLC, Ardmore, Oklahoma 73401, USA,*
[3]*Institute of Agricultural Biosciences, Oklahoma State University, Ardmore, Oklahoma 73401, USA,*
[4]*Sainsbury Laboratory, University of Cambridge, Cambridge CB2 1LR, UK,*
[5]*Shanghai Institute of Plant Physiology and Ecology, Shanghai 200032, China, and*
[6]*University of Queensland, Brisbane, Australia*

Received 10 September 2023; revised 27 November 2023; accepted 27 December 2023.
*For correspondence (e-mail m.udvardi@uq.edu.au).
The author responsible for distribution of materials integral to the findings presented in this article in accordance with the policy described in the Instructions for Authors is Michael Udvardi (m.udvardi@uq.edu.au).

SUMMARY

The conservation of GOLVEN (GLV)/ROOT MERISTEM GROWTH FACTOR (RGF) peptide encoding genes across plant genomes capable of forming roots or root-like structures underscores their potential significance in the terrestrial adaptation of plants. This study investigates the function and role of GOLVEN peptide-coding genes in *Medicago truncatula*. Five out of fifteen GLV/RGF genes were notably upregulated during nodule organogenesis and were differentially responsive to nitrogen deficiency and auxin treatment. Specifically, the expression of *MtGLV9* and *MtGLV10* at nodule initiation sites was contingent upon the NODULE INCEPTION transcription factor. Overexpression of these five nodule-induced GLV genes in hairy roots of *M. truncatula* and application of their synthetic peptide analogues led to a decrease in nodule count by 25–50%. Uniquely, the GOLVEN10 peptide altered the positioning of the first formed lateral root and nodule on the primary root axis, an observation we term 'noduletaxis'; this decreased the length of the lateral organ formation zone on roots. Histological section of roots treated with synthetic GOLVEN10 peptide revealed an increased cell number within the root cortical cell layers without a corresponding increase in cell length, leading to an elongation of the root likely introducing a spatiotemporal delay in organ formation. At the transcription level, the GOLVEN10 peptide suppressed expression of microtubule-related genes and exerted its effects by changing expression of a large subset of Auxin responsive genes. These findings advance our understanding of the molecular mechanisms by which GOLVEN peptides modulate root morphology, nodule ontogeny, and interactions with key transcriptional pathways.

Keywords: GOLVEN, ROOT MERISTEM GROWTH FACTOR, peptide hormones, root nodule symbiosis, lateral root.

INTRODUCTION

Root architectural responses to environmental cues such as availability of the macronutrient Nitrogen (N), are complex and there is much to learn about the mechanisms that control root plasticity (Lynch, 2019). Changes in root system architecture involve positioning, initiation and emergence of lateral organs that enable plants to respond dynamically to fluctuations in supply and demand of water and nutrients (Laskowski & Ten Tusscher, 2017). For example, 'rhizotaxis' ensures the correct placement and regular spacing of lateral roots. Plant roots demonstrate this deliberate underground architecture to optimize their nutrient acquisition strategies. The ability of legumes to form nodules, a second type of root lateral organ within which rhizobia convert atmospheric-N into plant-usable ammonia, adds another layer of complexity (Roy et al., 2020).

Plant hormones, including peptide hormones, are major determinants of root plasticity that bring about their

effects by synergistic and antagonistic interaction between signaling networks (Leyser, 2018; Matsuzaki et al., 2010; Meng et al., 2012; Roy & Muller, 2022; Whitford et al., 2012; Zhu et al., 2020). Peptide hormones are short chains of amino acids that upon binding with their cognate cell surface receptors initiate a signal relay that ultimately controls physiological responses (Roy & Muller, 2022). The biological activity of chemically synthesized peptides predicted from genome sequences has revolutionized the field of chemical genomics. This has led to the discovery of multiple novel peptide hormones and helped uncover their roles in plant growth and root development (de Bang et al., 2017; Matsuzaki et al., 2010; Okuda et al., 2009). Two well-known families of peptide hormones, namely CLAVATA3/ENDOSPERM SURROUNDING REGION (that includes *MtCLE12*, *MtCLE13*, *MtCLE34*, *MtCLE35* encoding prepropeptides) and C-terminally ENCODED PEPTIDE (example *MtCEP1*, *MtCEP7*), control lateral root and nodule development in *Medicago truncatula* (Imin et al., 2013; Mens et al., 2021; Moreau et al., 2021; Mortier et al., 2010). CEPs act as root-to-shoot 'N-hunger' signals controlling lateral root development and uptake of nitrogen in N-poor soils and in *M. truncatula* the shoot-acting LEUCINE RICH REPEAT- RECEPTOR LIKE KINASE (LRR-RLK) receptor named COMPACT ROOT ARCHITECTURE (MtCRA2), perceives MtCEP1 (Mohd-Radzman et al., 2016; Roy et al., 2022; Tabata et al., 2014). The CLE peptides are perceived by an LRR-RLK, SUPER NUMERIC NODULATION (SUNN)/-HYPERNODULATION ABERRANT ROOT FORMATION 1, downstream of which the microRNA *miR2111-5* targets the transcripts of the nodulation repressor *TOO MUCH LOVE* to optimize nodule number (Okamoto et al., 2013; Okuma et al., 2020; Roy et al., 2020). Together these two pathways maintain an optimal N-balance and control nodule number in legumes as part of a long-distance feedback loop called Autoregulation of Nodulation (AON) that restricts nodulation under N-replete conditions as well as N-deficient conditions (Laffont et al., 2020). Members of two additional post translationally modified peptide families, PHYTOSULFOKINE (LjPSK8) and GOLVEN/ROOT GROWTH FACTOR/-CLAVATA3 EMBRYO-SURROUNDING REGION LIKE (MtGLV9/MtRGF3) have also been implicated as positive and negative regulators of nodule formation, respectively (Li et al., 2020; Wang et al., 2015). While the roles of CLE and CEP peptides in root and nodule development are well-established, another class of peptides, the GOLVEN (GLV) peptides, offers additional insights into the intricate regulation of root growth and beneficial interactions with rhizobia.

The sulfated GOLVEN (GLV) peptides are known to control six root growth traits: cell number at the root meristem via activation of PLETHORA (PLT) transcription factors, which affects primary root growth (Matsuzaki et al., 2010); cell division during lateral root initiation thereby controlling lateral root density and patterning (Fernandez et al., 2015, 2020; Meng et al., 2012); auxin distribution via modulation of PIN efflux transporters thus regulating root gravitropism (Whitford et al., 2012); root cell number and circumferential cell growth rate under phosphate deficiency (Cederholm & Benfey, 2015); nodule number (Li et al., 2020), lateral root spacing (Jourquin et al., 2022) as well as defense responses (Li et al., 2023; Stegmann et al., 2022). At the molecular level, GLVs affect components of the auxin efflux transport pathway (PIN2) and auxin signaling (ARF7, ARF19) pathway and may reduce auxin concentrations at lateral root (LR) initiation sites (Fernandez et al., 2020; Whitford et al., 2012). Both nodule and lateral root formation are conditioned by changes in auxin flux and localized biosynthesis that lead to formation of local auxin maxima conducive for first cell divisions, organ initiation and outgrowth (Laskowski & Ten Tusscher, 2017; Leyser, 2018). During nodule formation, this auxin buildup is associated with the transcription factor NODULE INCEPTION (NIN) (Schiessl et al., 2019).

Chemically synthesized plant hormones such as Indole-3-Acetic acid (3-IAA) and 6-Benzyl-Aminopurine (6-BAP) are instrumental in elucidating physiological roles of the classical hormones auxin and cytokinin, respectively (Michniewicz et al., 2019). Chemical genetics and synthetic peptides are equally valuable for understanding the role of peptide hormones in plant responses to their environment. Notably, discovery of LURE peptide, CEP peptide, and CLE peptide activity were all facilitated by their synthetic counterparts (Corcilius et al., 2017; Goto et al., 2011; Laffont et al., 2020; Okuda et al., 2009). The model legume *M. truncatula* has over 1800 potential genome encoded peptides, of which less than twenty have been functionally characterized (Boschiero et al., 2020; de Bang et al., 2017). Even when non-peptide-coding genes are functionally studied, the assays used focus on three main phenotypes: rhizobial infection (structure and number of infection threads), nodule organogenesis (morphology and number of nodules), and N-fixation rates (measured by acetylene reduction assays) (Roy et al., 2020). An understudied aspect of root nodule symbiosis is control of nodule positioning. Penmetsa et al., observed that the radial position of nodule development relative to xylem and phloem poles were altered in Medicago *sickle* and *sunn* mutants (Penmetsa et al., 2003). Another hypernodulation mutant, *Ljplenty*, exhibited a wider zone along the primary root over which nodules were formed (Yoshida et al., 2010). In the current study, we investigated the biological role of nodule-induced GLVs and found that they decrease the length of the nodulation zone by altering nodule positioning along the primary root axis. We term this phenomenon 'nodule-taxis', by analogy to the term 'rhizotaxis' to describes the arrangement or positioning of nodules along the primary

root, which we also find to be under the influence of the GLV10 peptide.

RESULTS

GOLVEN peptide encoding genes are present in genomes of all plants that form roots or root-like organs

The legume *Medicago truncatula* encodes fifteen GOLVEN prepropeptide genes. To investigate neofunctionalization of *GLV* genes in legumes, we retrieved their orthologues from twenty-one species of the Fabales, Fagales, Cucurbitales, Rosales nodule-forming eurosids, the rosid and asterid clades of the eudicots as well as monocots, gymnosperms and basal lycophytes, bryophytes and chlorophytes (Figure 1; Figure S1, Table S1). All GLVs had putative orthologues in non-nodulating plant species suggesting no specialized roles during nodulation. However, although the *GLV* genes were present in plants that form roots or rhizoids, they were completely absent in the chlorophytes, which lack roots, such as *Chlamydomonas reinhardtii*, suggesting an evolutionary role in land colonization (Figure 1), (Furumizu et al., 2021). In contrast with Furumizu et al., we found putative GOLVEN orthologues in the lycophyte representative *Selaginella moellendorffii* genome, encoding putative thirteen amino acid long bioactive peptides (Figure 1; Table S1). This is noteworthy since the lycophyte clade represents the first lineage where roots arose compared to the rootless chlorophytes (Fang et al., 2021).

Members of the GOLVEN peptide family are transcriptionally regulated by plant nitrogen-status and during nodule development

To thoroughly investigate this gene family we next investigated their gene expression profiles. Using quantitative Polymerase Chain Reaction (qPCR) on nodule segments at 4, 10, 21 and 28 days post inoculation (dpi), we found that among the fifteen GLV family members, *MtGLV1*, *MtGLV2*, *MtGLV6*, *MtGLV9*, and *MtGLV10* show higher expression in nodules compared to roots across all analyzed nodulation stages (Figure 2a; Figure S2). Two *MtGLV1* orthologs in determinate nodule-forming Soybean (Glyma.02G079700 and Glyma.16G164100) also showed highly specific nodule expression (Figure S1). In Medicago roots, *MtGLV6*, *MtGLV9* and *MtGLV10* encoding genes were induced by short term N-deprivation stress (Figure 2a) compared to supply of optimal Nitrogen (4 mM NO_3^- + 2 mM NH_4^+) for 48 h but not for prolonged N-deprivation stress (Figure 2a; Figure S2). Expression of Arabidopsis GLVs were also altered in different zones of the root upon N-deprivation (Figure S3). However, pre-symbiotic regulation of N-deprivation induced GLVs in legumes could also allude to their function in early symbiosis stages such as dedifferentiation of root cortical cells and the regulation of early nodulin genes.

The transcription factor NIN regulates *MtGLV9* and *MtGLV10* expression during auxin-mediated nodule initiation

For lateral organ formation, it is essential to establish localized maxima of the hormone auxin. During nodulation, this establishment relies on the transcription factor NODULE INCEPTION (NIN) (Leyser, 2018; Schiessl et al., 2019). Since GLVs act by altering auxin transport and signaling in Arabidopsis roots (Fernandez et al., 2020; Whitford et al., 2012), we first tested whether their expression is regulated by auxin. Four of the five nodule-enhanced *GLVs* were upregulated in seedling roots treated with 1 μM Indole-3-acetic acid (3-IAA) 3 h post treatment (Figure 2b). To further investigate the relationship between GLVs and NIN in the context of auxin regulation during nodule initiation, we conducted experiments on nodulated roots. Using qPCR on spot inoculated root segments infected with *Sinorhizobium meliloti* strain 2011 (Sm2011) for 24 h, we detected that *MtGLV9* and *MtGLV10* transcripts were induced at nodule initiation sites in WT but not in *nin-1* mutants, indicating that induction of these genes is dependent on NIN (Figure 2c). Publicly available RNA sequencing data suggests expression of *MtGLV1*, *MtGLV2*, and *MtGLV6* was not dependent on NIN (Schiessl et al., 2019). These findings indicate that at nodule initiation sites, where auxin accumulation is an early step in nodule formation, *GLV9* and *GLV10* expression is dependent on NIN (Huo et al., 2006; Roy et al., 2017; Schiessl et al., 2019).

Five *GLV* genes exhibit overlapping expression patterns implicating redundant roles in nodule meristem maintenance

Spatial expression patterns obtained using promoter-GUS fusions in transgenic nodules corroborated our qRT-PCR expression data (Figure 3). The five nodulation-related *GLV* genes showed overlapping patterns of expression at sites of nodule initiation associated with successful infections and cell divisions suggesting they might act redundantly during nodule formation (Figure 3). Of the five genes, *MtGLV10* had the most confined expression pattern, being restricted to dividing cells underlying infection sites, while expression of *MtGLV1, MtGLV2* was associated with nodule vascular bundles closer to the nodule meristem (Figure 3a; Figure S2). None of the five genes were expressed in infected root hairs (Figure 3a; Figure S2). In mature nodules, expression of the GLVs was confined to the meristem, typical of genes involved in meristem maintenance as in Arabidopsis (Fernandez et al., 2015). We observed a similar but non-overlapping expression pattern of all five *GLV*s in initiating lateral roots (LRs) and the root tip. *MtGLV1* and *MtGLV10* were expressed in all dividing

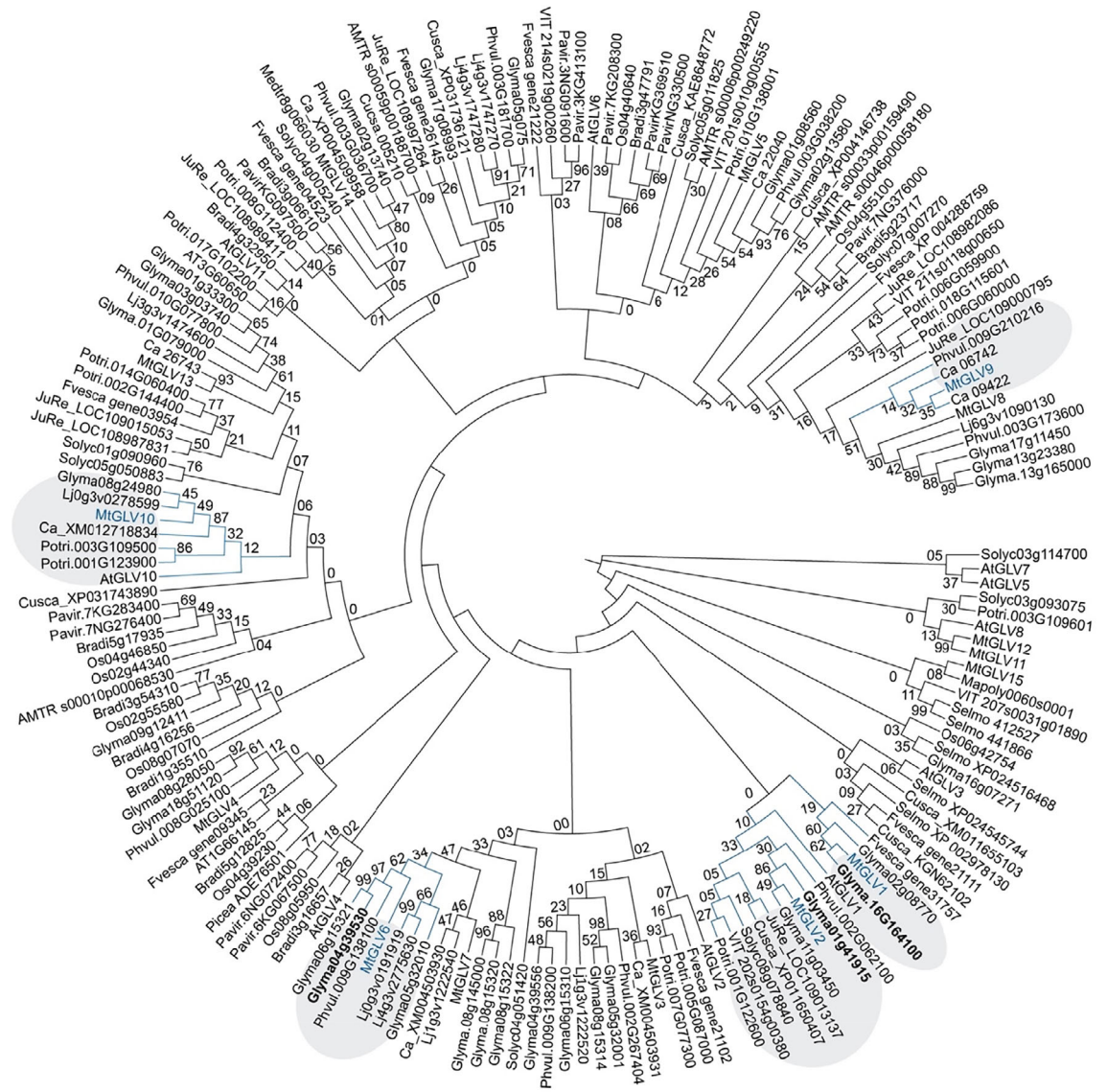

	Species	Number of homologs
Chlorophyte	*Chlamydomonas reinhardtii*	0
Bryophyte	*Marchantia polymorpha*	1
Lycophyte	*Selaginella moellendorffii*	5
Gymnosperm	*Picea sitchensis*	1
Angiosperm (basal)	*Amborella trichopoda*	5
Monocots	*Brachypodium distachyon*	10
Monocots	*Oryza sativa*	9
Monocots	*Panicum virgatum*	10

	Species	Number of homologs
Asterids - Solanales	*Solanum lycopersicum*	9
Rosids - Vitales	*Vitis vinifera*	5
Eurosids - Brassicales	*Arabidopsis thaliana*	13
Eurosids - Malphigiales	*Populus trichocarpa*	14
Eurosids - Fabales	*Cicer arietinum*	8
Eurosids - Fabales	*Glycine max*	30
Eurosids - Fabales	*Lotus japonicus*	9
Eurosids - Fabales	*Medicago truncatula*	15
Eurosids - Fabales	*Phaseolus vulgaris*	11
Eurosids - Fagales	*Juglans regia*	7
Eurosids - Cucurbitales	*Cucumis sativus*	8
Eurosids - Rosales	*Fragaria vesca*	9

Figure 1. GOLVEN like peptides are encoded in all plants that form roots or root-like structures.
Maximum likelihood phylogenetic tree created with the full length GOLVEN encoding polypeptide using MEGA X with 1000 bootstraps each. Please refer to Table S1 for gene IDs and corresponding peptide sequence.

cells of the LR while *MtGLV2*, *MtGLV6*, *MtGLV9* were expressed on the flanks of LR primordia. At the root tip, *MtGLV9* and *MtGLV10* were expressed in columella cells, *MtGLV1*, *MtGLV2* were expressed in root cap cells and *MtGLV6* was expressed in the lateral root cap cells (Figure 3a).

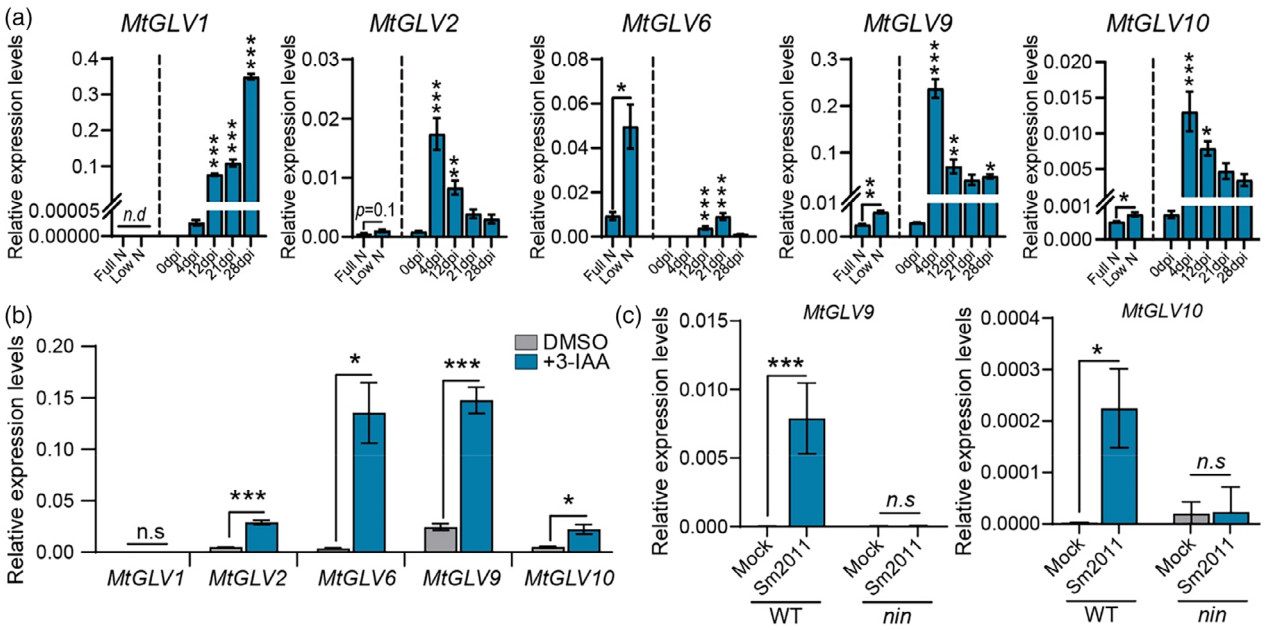

Figure 2. Expression of GOLVEN/ROOT GROWTH FACTOR peptide-coding genes is induced during nitrogen deficiency, auxin treatments and root nodule symbiosis.

(a) Bar charts showing quantitative-PCR estimation of transcript abundance after 48 h of nitrogen deprivation and at different time points (days post inoculation) during nodule development compared to uninfected roots (0 dpi). Error bars depict standard error of mean.

(b) Bar charts showing quantitative-PCR estimation of transcript abundance in *M. truncatula* seedling roots treated with 1 μM auxin (3-IAA) or the solvent control (DMSO). Data are representative of three biological replicates with 40–60 seedling roots per replicate. Error bars depict standard error of mean.

(c) Bar charts showing quantitative-PCR estimation of MtGLV9 and MtGLV10 transcript abundance in spot inoculated nodules on *M. truncatula* WT and *nin* mutants. Data are representative of three biological replicates each with at least 50–60 spot inoculated nodules. $*P < 0.05$, $**P < 0.01$, $***P < 0.001$.

Overexpression of five nodule-induced *GOLVEN* genes negatively regulates nodule number

Next, to determine effects of GLV peptides on nodulation, we cloned the coding regions of *MtGLV1*, *MtGLV2*, *MtGLV6*, *MtGLV9* and *MtGLV10*, downstream of the Lotus *UBIQUITIN* promoter and generated transgenic hairy roots, via *Agrobacterium rhizogenes*-mediated transformation (Maekawa et al., 2008). We included a clone with a single base pair deletion in the coding region of *MtGLV9* (+203 bps from ATG) as a negative control along with an empty vector overexpressing the *GUS* gene. Overexpression of the *GLV* genes reduced the number of nodules formed on transformed roots 21 dpi by 25–50% (Figure 4; Figure S5). *MtGLV9* and *MtGLV10* had the strongest inhibitory effects on nodulation whereas the mutated *mMtGLV9* had no significant effect on nodulation. These findings indicated that overexpression of GLVs can deregulate optimal nodule formation.

Synthetic GOLVEN peptides regulate several root growth parameters including the position of the first nodule

To determine if externally applied synthetic peptides phenocopied GLV function *in planta* we took a chemical genetics approach to explore the role of GLVs in root nodule symbiosis and control of root architecture traits (Figure S6). We synthesized GLV peptide variants and measured their effects on root growth parameters and nodulation traits to identify the synthetic peptide with the strongest, most reproducible effects for further investigative studies. Peptides predicted to be encoded at the C-terminal domain of *MtGLV1*, *MtGLV2*, *MtGLV6*, *MtGLV9* and, *MtGLV10*, immediately following the peptidase cleavage recognition motif 'DY' were synthesized (Figure S3). Phenotypic effects of the peptides GLV1p, GLV2p, GLV6_hyp9p, GLV6_hyp10p, GLV9p, and GLV10p carrying a modified sulfotyrosine at position two, applied at 1 μM concentration, were distinct from those of scrambled, unmodified and unsulfated GLV10p, and solvent controls (Figure 5a,b). These results reinforce previous studies that show sulfation of the tyrosine at position two is essential for GOLVEN peptide activity (Matsuzaki et al., 2010). Since the Autoregulation of Nodulation is a well characterized pathway affecting total nodule number, we tested effects of the GLV10 peptide on *sunn* (*SUPERNUMERIC NODULES*) mutants (Figure S7). The *sunn* mutants retained sensitivity to the peptide suggesting that for nodule number control, the AON pathway and GLV control of organogenesis act separately.

We tested eighteen root growth parameters and found that GLV peptides significantly affected at least ten of them (see Table S2). Similar to observations in Arabidopsis, GLV

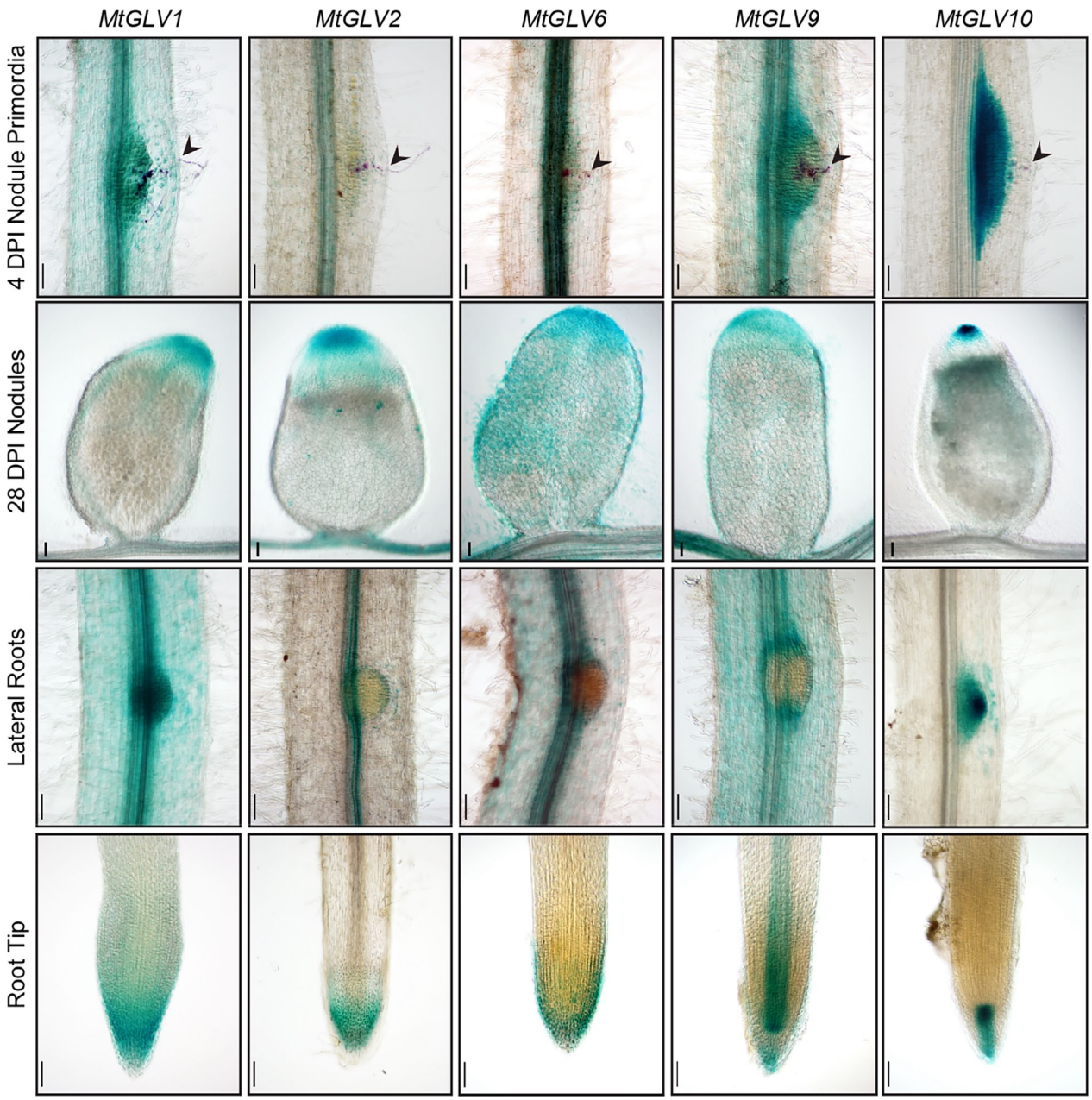

Figure 3. Five GOLVEN/ROOT GROWTH FACTOR peptide-coding genes are expressed during nodule organogenesis and root growth.
Promoter-GUS reporter fusions showing spatial expression of nodule-induced *GLV* peptide-coding genes in nodule primordia, mature nodules, lateral roots and root tips. Arrowheads indicate infection threads. Scale bars denote 100 μM except for mature nodules (28 DPI) which measure 500 μM. At least 4–6 independent hairy root lines were assessed at every time point.

peptides promoted primary root growth/length (Figure 5a). Furthermore, the roots displayed varying degrees of agravitropism, with GLV10p effects being the most pronounced (Figure S6; Figure 5a) (Matsuzaki et al., 2010; Meng et al., 2012; Whitford et al., 2012). However, while there was a positive influence on root length, several GLV peptides, including GLV1p, GLV2p, GLV6_hyp9p, GLV6_hyp10p, GLV9p, and GLV10p, negatively affected lateral organs such as lateral roots (LRs) and nodules. This impact was evident in both the number and density of these organs along the primary root (Figure 5b). A clustering analysis further highlighted that GLV9p and GLV10p had the most similar effects on root growth phenotypes (Figure 5b). Notably, these peptides didn't influence the growth rates of *S. meliloti* Rm2011 over 60 h. This suggests that the observed nodulation phenotypes are likely a direct effect on the plant, not its

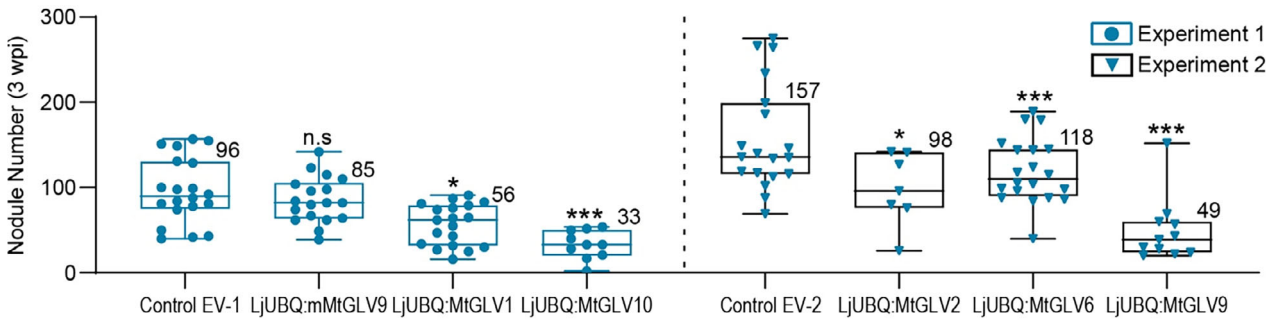

Figure 4. Overexpression of all five *GLV* coding genes in hairy roots of *M. truncatula* suppresses the formation of nodules.
Each individual dot or triangle in the box plot indicates an independent line. Average nodule number of indicates on the shoulder of each box plot. One-way ANOVA followed by Dunnett's multiple comparison test was performed separately for experiment 1 and experiment 2 with their respective controls where $*P < 0.05$, $**P < 0.01$, $***P < 0.001$. Data displayed summarize two independent experiments per construct. Average values are provided on the shoulder of each box plot.

associated microsymbiont (Figure S3d). Interestingly, there was a shift in the position of the basal-most nodule (the developmentally oldest nodule, Trait 16) in relation to the primary root length upon GLV10p treatment. This meant that nodules began initiating further along the primary root (Figure 5c). This resulted in a reduced absolute length of the zone over which nodules initiated (Nod zone, Trait 18) (Figure 5c).

Since nodulation and rhizobial infections are genetically distinct but related processes, we tested effects of the peptides on early infection structure development. GLV peptides reduced the total root length, including secondary and tertiary LRs, as well as the total number of early infection events (Figure S3). However, the GLVs did not affect early infection initiation events per cm root, except for GLV10p, which resulted in more microcolonies and infection thread initiations, but a strong reduction in nodule formation (Figure S3). Increased infection induced by GLV10p may have been a consequence of the severe reduction of nodule number, as observed for symbiotic mutants with colonization defects such as *nf-ya1* (Laporte et al., 2014). As GLV peptides did not seem to affect infection directly but reduced nodule density, we focused on their effects on root cortical processes such as organogenesis.

Alteration of the nodule position by GLV10 controls the zone of lateral organ formation

Lateral root positioning (rhizotaxis) is an understudied trait while nodule positioning over the longitudinal root axis (we term noduletaxis) has not been described in literature before. Therefore, we further investigated these two traits. In Arabidopsis, periodic pulses of auxin-induced gene expression occur over a zone of the root close to the root tip called the 'oscillation zone' which pre-patterns longitudinal spacing or LR primordia positioning and consequently determines the zone of the root that is primed or capable of initiating lateral roots (Hofhuis et al., 2013; Laskowski & Ten Tusscher, 2017). To better understand the effect of GLV peptides on lateral organ positioning (Traits 16–18), we pursued the peptide with the strongest and most reproducible effect, that is, GLV10p (Figure 6c). In untreated seedlings, nodules typically originated at the midpoint (50%) relative to the length of the primary root. Upon GLV10p treatment, the position of the first nodule shifted to approximately 60% of the primary root length (Figure 6a,c). Similarly, the relative position of the first lateral root was lower on the primary root, while that of the developmentally last formed root primordia appeared to be proximal to the root base (Figure 6a). This shift in organ positioning resulted in a statistically significant reduction of the absolute length of the root over which nodules formed (nod zone) and the zone that supported lateral roots (LR Zone, Figure 6b,d). In cases where there were only two nodules on the main root, the distance between two successive nodules was reduced. We tested the effect of GLV10p peptide effects over the 1–10 μM range on WT *M. truncatula* seedlings (Figure S8) and found that effects were detectable even at a concentration of 100 nM up to 1 nM, depending on the trait under study.

In *A. thaliana*, GLV peptides are perceived by five LRR-RLKs *ROOT GROWTH FACTOR1 INSENSITIVE/ROOT GROWTH FACTOR RECEPTOR*, namely AtRGI1/AtRGFR1, AtRGI2/AtRGFR2, AtRGI3/AtRGFR3, AtRGI4, and AtRGI5. The Arabidopsis *rgfr1 rgfr2 rgfr3* triple mutant has a stunted primary root and an enlarged root meristem but retains sensitivity to GLV peptide with respect to LR density (Shinohara et al., 2016). We tested the effect of Medicago GLV10p on Arabidopsis root growth. GLV10p, which has three amino acids different from AtGLV10p, was perceived by Arabidopsis roots and, as in Medicago, shifted the relative position of the first lateral root to a more distal position on the primary root and decreased the zone of LR formation (Figure S4a,b). However, the triple *rgfr* mutant was insensitive to GLV10p peptide with respect to LR positioning and LR zone (Figure S4a), indicating that the effect of the peptide on LR zone formation was dependent on the RGI receptors. Using the synthetic AtGLV10 peptide yielded strong effects on Arabidopsis plants, with the *rgfr* mutants

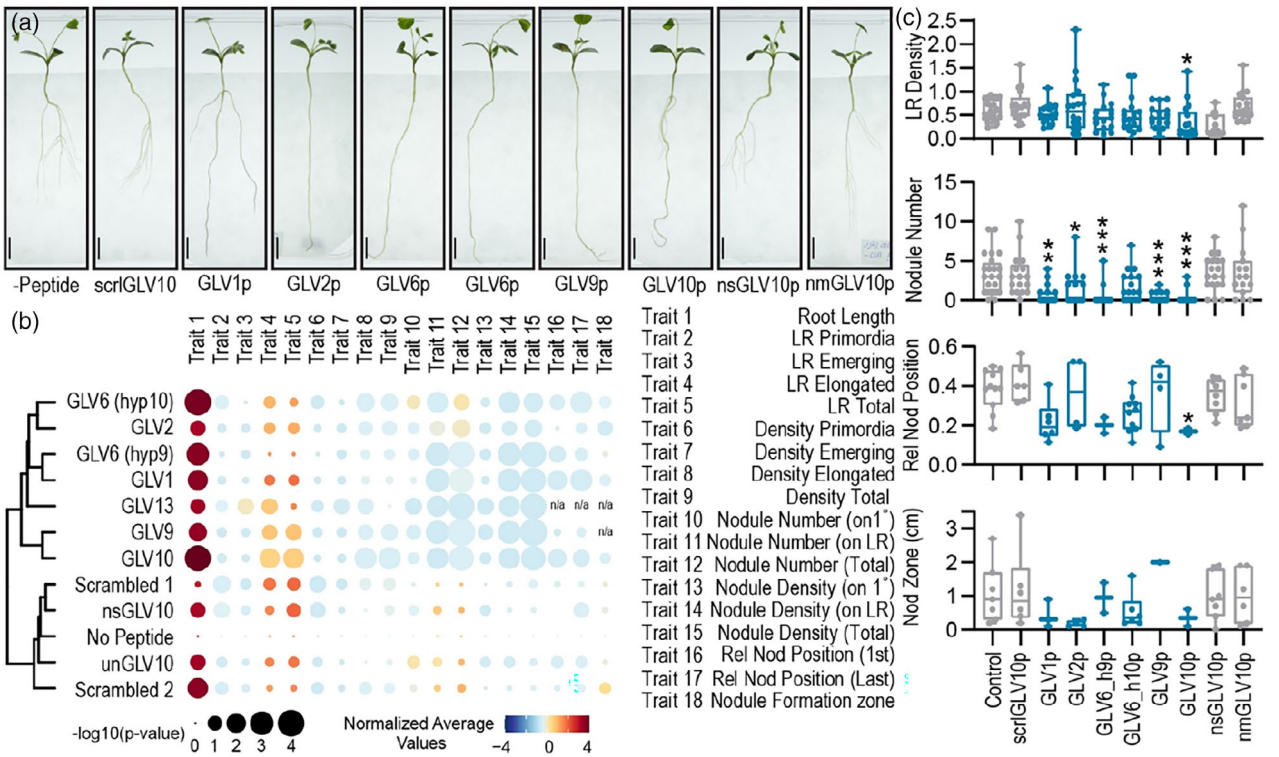

Figure 5. GLV peptides affect root architecture and nodule formation.
(a) Representative images showing *M. truncatula* Jemalong A17 seedlings 10 days post germination (dpg) on plates containing 1 μM of the indicated peptide in B&D medium with 0.5 mM KNO3. The predicted bioactive peptides (GLVp) were around 13 amino acid residues long except for GLV2p (Figure S2). Peptides were synthesized with a sulfotyrosine residue at position two and a hydroxyproline at position ten. In case of MtGLV6 where there was more than one proline, we designed alternate versions with a hydroxyproline in either position 9 (GLV10_hyp9) or 10 (GLV10_hyp10). A synthetic version of MtGLV13 derived peptide, which was not regulated during nodulation, was included. As negative controls we generated a non-modified (non-sulfated, non-hydroxylated) version of the most potent peptide GLV10p (nmGLV10) and a hydroxylated non-sulfated version (nsGLV10). We generated a 'scrambled' version of MtGLV10 (scrlGLV10) with identical amino acid composition but a randomized order of amino acids with or without the secondary group modifications (Refer to Extended Data Figure 2 for corresponding peptide sequences).
(b) Corresponding rain plot showing cumulative growth data of seedlings 10 dpi with *Sinorhizobium meliloti* Rm 2011 dsRED. Colors represent normalized average values with red representing increased trait values and blue representing decreased trait values. Data were compared using a Student's *t*-test and bubble size indicates −log (*P*-value). Refer to Table S1 for trait definitions.
(c) Boxplots of four individual traits of interest showing effect of GLV peptides compared to negative controls; Trait 9 (Total LR density), Trait 12 (Total nodule number), Trait 16 (Relative position of first formed nodule), Trait 18 (Nodule formation zone). Asterisks represent $*P < 0.05$, $**P < 0.01$, $***P < 0.001$ using a Brown-Forsythe and Welch ANOVA-protected Dunnett's multiple comparison test (treatment vs no-peptide control).

showing either no response or a response opposite to that observed in wild type plants (Figure S9); phenotypes suggesting the signaling pathway is no longer functional.

Finally, to test whether these effects were also mediated by GLV10 *in planta* we isolated homozygous mutants of *MtGLV10, glv10-1* (NF12742) and *glv10-2* (NF20983), with exonic insertions of the *Tnt1* retrotransposon (Figure S5) (Tadege et al., 2008). The lateral root zone appeared to be wider than the WT for *glv10-1* and *glv10-2*, but varied between alleles for the Nod zone (Figure 6e,f) and additional root growth phenotypes (Figure S10). Since there are several other GLV encoding genes involved in nodulation, higher order mutants are necessary for characterizing these traits in depth. Taken together, these data indicate that GLV peptides are regulators of lateral root zone formation and that this may be dependent on RGFR receptors. Mutants of orthologous genes in Medicago will shed light on their regulation during root nodule symbiosis.

Increased primary root growth upon GLV10 application is mediated by an increase in cell number per cortical cell file but not cell length

The spatial distribution of LRs or rhizotaxis is determined by a combination of three factors – primary root growth, organ density and the distance between successive organs (Du & Scheres, 2018). Studies in Arabidopsis show that application of AtGLV6 peptide to roots disrupts early symmetrical cell divisions required for correct lateral root initiation (Fernandez et al., 2020). Application of the peptide GLV10 increases root length and decreases lateral root density along the primary root both, in Arabidopsis and Medicago (Figure 5b,c). GOLVENs, therefore, control at

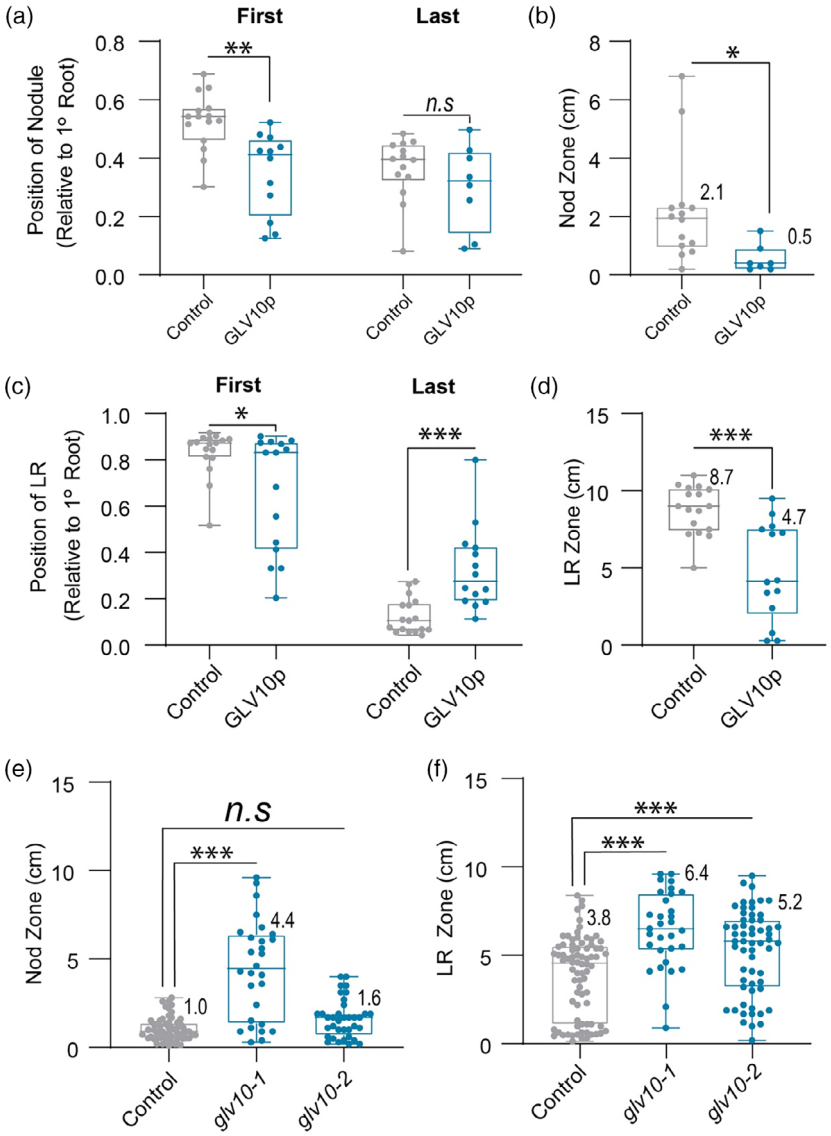

Figure 6. Peptide GOLVEN10 shifts the position of lateral organs consequently reducing the longitudinal zone of organ formation.
Position of the developmentally first and last formed organ relative to the primary root length measured from the root tip with and without GLV10p treatment and the resulting zone of organ formation on M. truncatula Jemalong A17 seedlings 14 dpi with Sm2011 dsRED and 17 days post germination.
(a) Nodule position (b) Nodule formation zone (c) Lateral root position (d) LR formation zone. Asterisks represent $*P < 0.05$, $**P < 0.01$, $***P < 0.001$ using a Student's *t*-test.
(e.f) Size of the Nod Zone and LR Zone in WT R108 compared to single glv9 and glv10 mutants two wpi with Rm2011. Data are representative of cumulative values from two identical experiments. Asterisks represent $*P < 0.05$, $**P < 0.01$, $***P < 0.001$ using ANOVA-protected Dunnett's multiple comparison test. Numeric values for the absolute zone of lateral organ formation are provided on the shoulder of box plots.

least two of the three factors responsible for spatiotemporal organ positioning. To understand the cellular basis of GLV10 mediated root elongation in Medicago we collected longitudinal sections of roots 1 cm above the root tip which revealed that cell number and cell size and cell organization were affected by application of GLV10 (Figure 7a). While cell length along the longitudinal axis decreased by more than 50%, the cell number per cortical cell file increased by 50% (Figure 7b); this effect persisted even in mature regions of the root (Figure S11). Multicellular processes such as root growth are dependent on the combined activity of two linked processes, cell expansion and cell division (Jones et al., 2019). Faster root elongation rates are correlated with increased cell division at the root meristem, with little change in cellular expansion rates (Beemster & Baskin, 1998). In keeping with this observation, we propose that an increase in cortical cell number caused by GLV10 plays a role in regulating root tissue

growth and consequently lateral organ positioning (Figure 7c).

Application of GLV10 impacts the root cytoskeleton and auxin pathway related genes

To uncover the underlying mechanisms of GLV10 peptide's effect on cell division and expansion, we sought to explore the transcriptomic changes induced by the peptide. Additionally, we were interested in discerning if the peptide had any impact on genes associated with nodulation. Differential gene expression analysis of three-day-old seedling roots comparing peptide-treated and untreated controls, identified 1091 GLV10p-genes induced and 787 repressed genes (Table S3), using a threshold of 1.5 fold change (0.58 log2 fold) and a *P*-value of less than 0.05 (Table S3). Gene Ontology (GO) enrichment analyses using Legume IPv3, revealed that the peptide most significantly repressed cytoskeletal and cell cycle processes while inducing genes related to hormone regulation (Figure 8a).

Among the downregulated genes, were three TPX2 (Medtr4g078565) and TPXL5-like genes (Medtr7g013070, Medtr6g015010), the MtAURORA1 kinase (Medtr3g110405) and ten kinesin genes including orthologs of *AtKINESIN* 12-E (AT3G44050, Medtr2g087840) (Figure 8b; Table S4) (Gao et al., 2022; Herrmann et al., 2021; Nishihama et al., 2002). The proteins encoded by these genes are vital for accurate cell division and the necessary cytoskeletal adaptations during this process. The typical TPX2 peptide has an N-terminal Aurora-binding hydrophobic domain, a median domain that binds importin, and a C-terminal segment characteristic of TPX2 that interacts with kinesins. Genes upregulated by GLV10 included regulators of salicylic acid (SAR DEFICIENT1, Medtr6g083320, Medtr8g104510, Medtr6g083810, Medtr6g083730), jasmonic acid (SUPPRESSOR OF NPH4 2, Medtr5g020020), cytokinin (CYTOKININ OXIDASE 3, Medtr4g126150), gibberellic acid (GIBERELLIC 2 OXIDASE, Medtr8g037310), brassinosteroid and abscisic acid (Table S4).

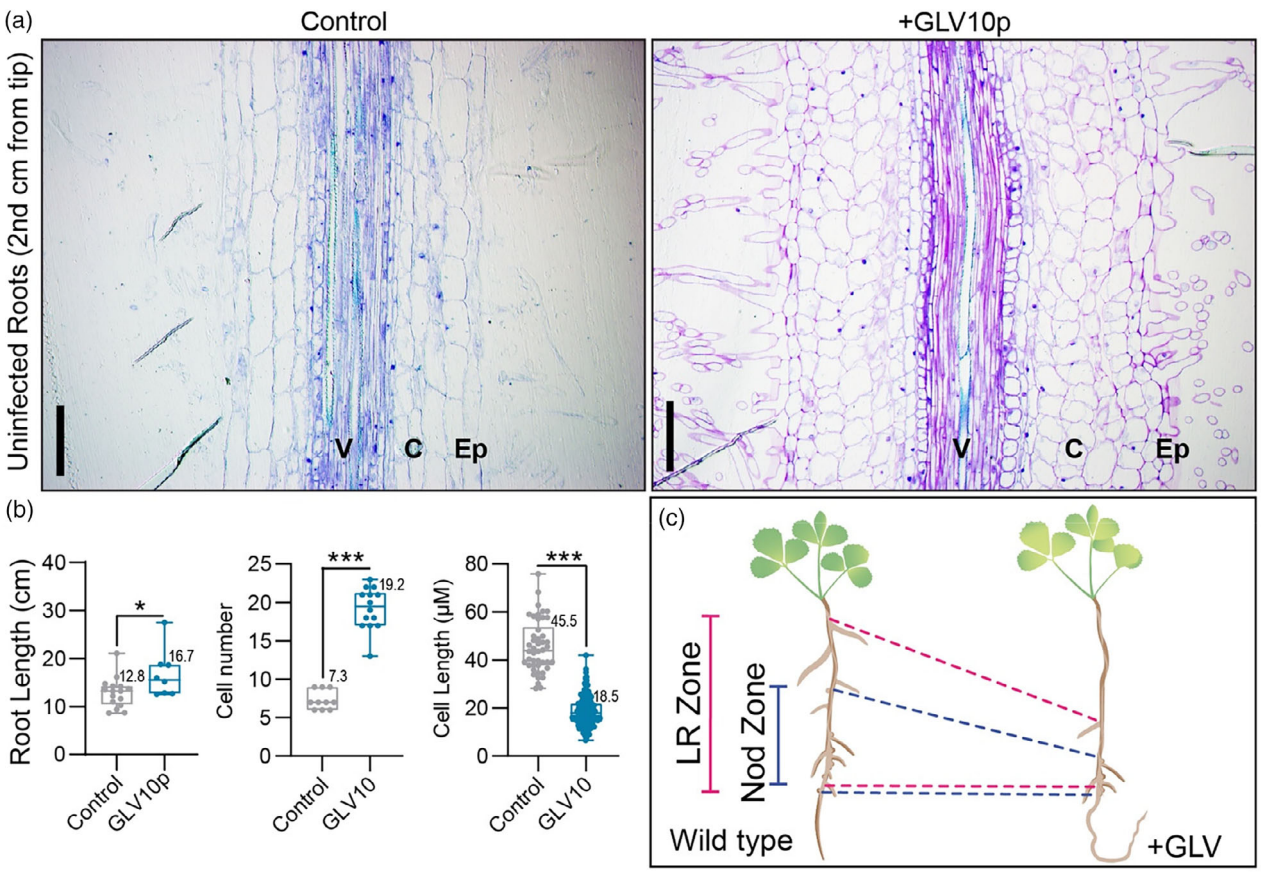

Figure 7. The synthetic peptide GLV10 affects cell number and cell size in Medicago roots.
(a) Images show 2.5 μm thick sections of root segments collected one cm below root tip at a 20× magnification. Control roots treated with solvent (left) and roots treated with 1 μM GLV10 peptide (right) for 7 days. Scale bars represent 50 μm. Segments from at least eight roots per sample were analyzed.
(b) Quantification of data shown in (a) using ImageJ. Application of GLV10 peptide increases root length by increasing cell number but decreasing cell size in each cortical cell file. Roots were treated with peptide for 7 days on plates and compared to untreated roots. Student's *t*-test $*P < 0.05$, $***P < 0.001$.
(c) Diagrammatic representation of nodulotaxy as mediated by the peptide GLV10.

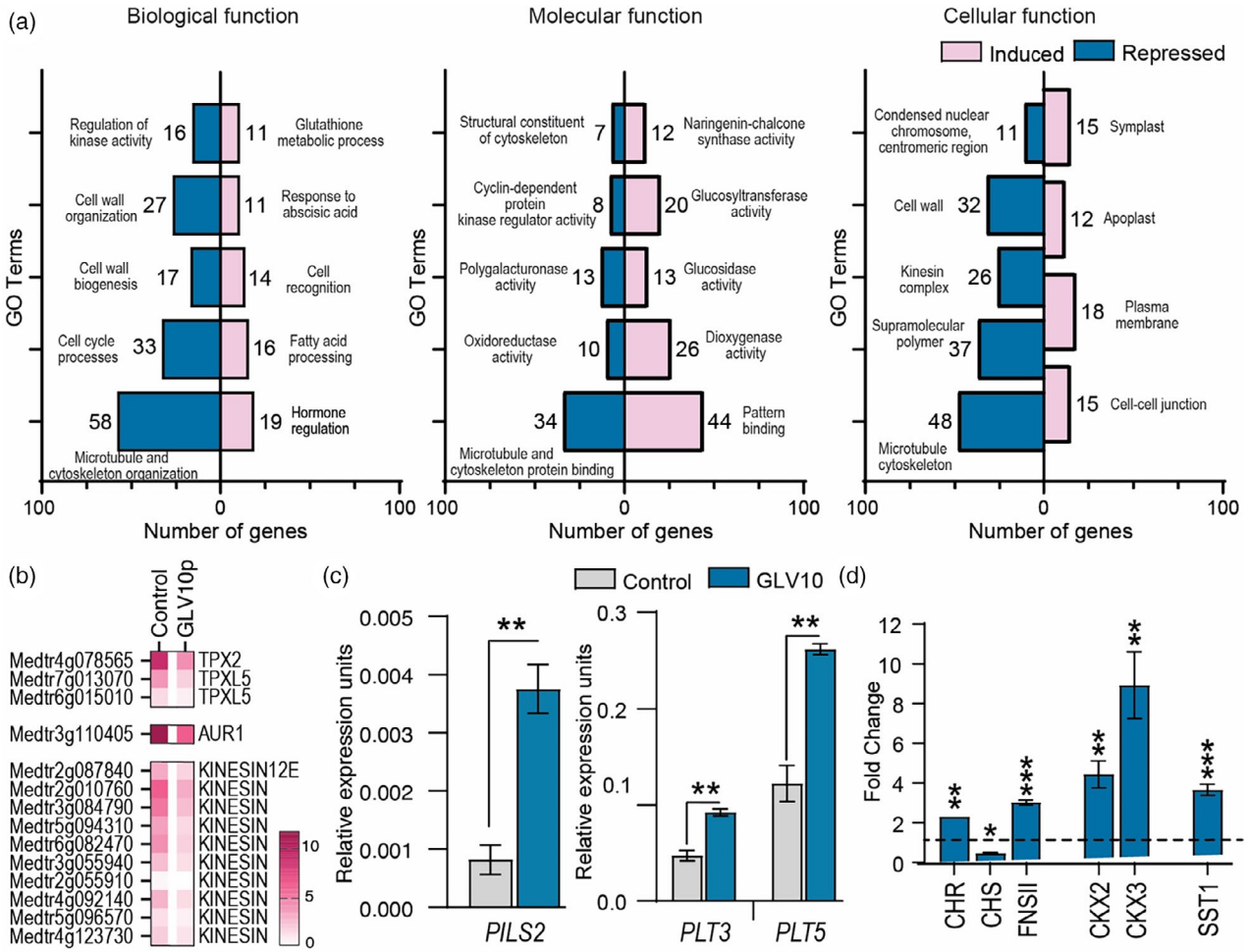

Figure 8. Transcriptomic analysis of GLV10 treated *M. truncatula* seedling roots.
(a) Bar charts showing GO categories enriched in GLV10 peptide-treated roots compared to control (water) treated seedlings 3 h post treatment. Additional GO numbers provided in Table S4.
(b) Heatmap showing enrichment of TPX2 like, AURORA1, Kinesin related genes that are downregulated in *M. truncatula* seedling roots 3 h post GLV10 peptide treatment.
(c) Quantitative RT-PCR estimation of GLV10 marker genes *MtPLT3* and *MtPLT5* and the PIN-LIKE auxin exporter *MtPILS2*.
(d) qPCR confirmation of nodulation marker genes differentially regulated by application of GLV10 peptide. Gene expression was normalized to two housekeeping genes *UBQ* and *PTB*. All gene ID's are provided in Table S3. Students *t*-test $*P < 0.05$, $**P < 0.01$, $***P < 0.001$.

Given that the phenotype observed after GLV peptide treatment resembled that of auxin-deficient mutants, we hypothesized that GLV10 may exert its effects by modulating auxin signaling, transport, and biosynthesis (Roy et al., 2017). We, therefore, compared the transcriptomic signature of GLV10 treated roots with that of publicly available RNA-Seq data of roots treated with the auxin Indole-3-acetic acid under identical conditions (Table S3, Figure S8). We found a 30% overlap between genes regulated by both, that is, 588 shared genes of 1878 genes regulated by GLV10 were also regulated by 3-IAA. These corresponds to a ~ 20% overlap between genes co-induced and those that are functionally antagonistic (Figure S12). The peptide transcriptionally regulated several *Aux-IAA*, *SAUR* and *GH3* genes which we confirmed by qPCR (Table S5, Figure S12). Interestingly, we found that in addition to GLV10p induction of PIN transporters, expression of the PIN-LIKE auxin exporter, *MtPILS2* (despite being lower than the log2-fold change of 0.58 that was used in this study) served as a reproducible marker of GLV10p activity (Figure 8b; Table S5).

Finally, comparison of differentially expressed genes (DEGs) with functionally characterized nodulation genes revealed that 18 crucial nodulation genes are regulated by GLVs (Table S3, Roy et al., 2020). Of these, members of the flavonoid pathway (*MtCHR*, *MtFNSII*), the cytokinin signaling pathway (*MtCKX2*, *MtCKX3*), and the PLETHORA transcription factors (*MtPLT3* and *MtPLT5*) were overrepresented among induced genes (Table S3; Figure 8b). In Arabidopsis, auxin-inducible *PLT*s are

regulated by GLVs and control meristem maintenance and root growth.

DISCUSSION

This study provides a thorough investigation of the GOLVEN multigenic peptide family using a combination of plant physiology, molecular biological and omics techniques. The conservation of the GLV peptides across land plants underscores their fundamental role in root development. Findings described herein suggest that while peptides within the same family may influence developmental processes in similar ways, the upstream regulatory mechanisms governing them can vary. Given that lateral roots and nodule organogenetic processes share >90% of genes (Schiessl et al., 2019), our data indicate that GLV peptides also likely got co-opted into nodule organogenesis downstream of the transcription factor NIN, thereby acquiring additional roles in legumes.

Role of GOLVENs in N-starvation and root development

When nitrogen availability is low, plants require an internal signal(s) to inhibit LR production and promote primary root elongation in search of deeper, N-rich soil layers. *MtGLV10* and *MtGLV9* are peptide hormones induced in roots upon short term N-starvation that act as negative regulators of LR initiation and positive regulators of root elongation (Figures 1a and 4b,c) phenocopying the N-starvation root architecture response (Mohd-Radzman et al., 2013). Modulation of root system architecture by GLVs in conjunction with auxin (Figure 1b) may have been instrumental in colonization of land by plants, allowing them to integrate nutrient stress signals into root developmental programs, given that GLVs are conserved in all land plants but not in rootless chlorophytes (Figure 3). Our data suggest that at least five GOLVEN peptide-coding genes act in concert to control root nodule symbiosis and root architecture traits (Figures 1 and 2). Of these five, MtGLV10 acts not only at the lateral organ initiation stage but earlier, likely during priming and organ positioning, which determines the zone of the root over which lateral organs can initiate and then emerge (Figures 4 and 5). We apply the definition of the 'Nodulation Zone', as defined by Yoshida et al., as the zone along the longitudinal root axis that is capable of undergoing cell division and supporting formation of nodules (Yoshida et al., 2010). Similarly, the Lateral Root Zone, as interpreted in this study describes the zone along the longitudinal root axis that is capable of undergoing cell division leading to initiation of lateral roots. The five nodule-induced peptides are activated during nodule organogenesis, but their regulation varies in response to factors such as auxin, nitrogen deficiency, and the symbiosis transcription factor NIN. For example, the expression pattern of *MtGLV1* was distinct from the other four genes, as it did not show induction under low nitrogen conditions or regulation by 3-IAA at the tested time point (Figure 2). Auxin self-modulates its signaling pathway through feedback loops, which involve the degradation of AUX/IAA proteins (Leyser, 2018). Consequently, such complex feedback mechanisms could account for the observed lack of induction of *MtGLV1* by 3-IAA at 3 h post treatment, potentially due to a variation in its temporal transcription response. The lack of response to low nitrogen levels raises several possibilities including one that MtGLV1 may integrate signals from other nutrient deficiencies, such as phosphorus, which are known to influence nodule formation (Isidra-Arellano et al., 2020). While the GLVs might have redundant roles during any one root organogenetic process and can compensate for their activity in the absence of any one of the peptides, expression of each peptide-coding gene is uniquely regulated. Different environmental signals or transcriptional regulators might, therefore, drive their roles in distinct root growth and nodulation processes.

Placing GLVs downstream of the symbiosis signaling pathway

Low soil-N (<1 mM N) availability promotes root nodule symbiosis, while simultaneously inducing the expression of *GLV*s that, ultimately, limit excessive nodulation (Figure 1a). Both, low N in roots and nodule development lead to GLV production in these organs similar to known Autoregulation of Nodulation pathway where CLE-SUNN signaling ensures sufficient but not excessive nodulation (Nishida et al., 2018; Okamoto et al., 2013). MtNIN directly stimulates the expression of *MtCLE13* prepropeptide. Once expressed, the MtCLE13 peptide is recognized by MtSUNN in the shoot, leading to the mediation of systemic AON which then restricts additional nodulation (Laffont et al., 2020). Our data indicate that in addition to controlling the CLE (and CEP) nodulation regulators (Laffont et al., 2020), NIN is required for *MtGLV9 and MtGLV10* expression at nodule initiation sites (Figure 1c). Identification of GLV receptor(s) will enable investigations into possible crosstalk with the CLE-SUNN module that regulates nodule number through long-distance signaling, or other root components such as SKL that control nodule number and positioning locally. Given that the *A. thaliana rgfr* triple mutant is insensitive to high doses of GLV10 peptide, which normally reduces the LR zone and alters LR positioning (Figure 5e,f), the corresponding receptor orthologues in *M. truncatula* are interesting candidates for further investigations. These include *AtRGFR1/ RGF1 INSENSITIVE 1* (*AtRGI*) (AT3G24240 putative orthologs Medtr5g045910), *AtRGFR2/AtRGI2* (AT5G48940 putative orthologs Medtr7 g059285 and Medtr3g090480), *AtRGFR3/AtRGI3* (AT4G26540 putative orthologs Medtr3g060880 and Medtr4g105370), *AtRGI4* (AT5G56040 putative ortholog Medtr5g096530) and *AtRGI5* (AT1G34110 putative ortholog Medtr1g097580) (Roy & Muller, 2022). The substantial upregulation of *MtRGFR1* (Medtr5g045910,

Mtsspdb.zhaolab.org) expression and repression of *MtRGFR3* (Medtr3g060880) in developing nodules implies their predominant role as the receptor isoforms in nodulation, although additional genetic studies are warranted to confirm this.

Noduletaxis and the nodulation zone

Like rhizotaxis, a phenomenon which ensures LR positioning and regular spacing between successive LRs, we find that a similar mechanism exists for nodule spacing, which we call noduletaxis (Figure 4a,b). Although nodules can cluster together at a particular infection site, they are typically spaced out along the longitudinal root axis or the nodulation zone. Such spacing is lost, however, in the *sickle* mutant that forms a continuous chain of nodule primordia, many of which fail to develop into functional nodules (Penmetsa et al., 2003; Penmetsa & Cook, 1997). Thus, mechanisms controlling nodule positioning and priming are important to ensure formation of fully developed, functional nodules. At present, rhizobial infection, nodule number and N-fixation efficiency are the predominant phenotypic traits that are measured when trying to understand gene function during root nodule symbiosis. Noduletaxis as a trait is rarely considered, if not completely overlooked, but is nevertheless important to restrict nodule numbers to levels that can be supported effectively by plant photosynthesis. Our study identifies GLV10 as a dual regulator of both rhizotaxis and noduletaxis that controls the zone of lateral organ formation in *M. truncatula*. Shifting the position of the first lateral organ more distal to the root base requires deferred organ initiation in space and/or in time. From studies in Arabidopsis, we know that GLV peptides disrupt initial cell divisions in the root pericycle, which delays or halts lateral root initiation (Fernandez et al., 2015, 2020). We found that in *M. truncatula*, another factor that contributes to this delay is faster root growth upon GLV application caused by an increase in cell number along the longitudinal root axis (Figure 6b). Both Nodules and LRs initiate acropetally, and no new organs develop between already developed lateral organs (Dubrovsky et al., 2006). In theory, if treated roots are longer than those of control plants at the time of organ initiation, which only occurs in a narrow zone of the root close to the Root Apical Meristem, the first formed lateral organ will initiate more distally from the shoot compared to untreated controls. Rapid cell division stimulated by GLV10 accelerates root growth rates thereby spatially shifting the position of the first lateral organ formed (Figure 5). Since organ positioning is determined by a combination of three factors, that is, primary root length, organ density and the distance between successive organs (Du & Scheres, 2018), further temporal delay in initiation of subsequent lateral organs would facilitate an overall decrease in the LR zone length or Nod zone length caused by altered cell division at organ initiation sites (Fernandez et al., 2015). Fixed or flexible threshold theory for cell division which proposes that cells undergo division only after they have reached a certain threshold of size, would suggest that smaller cells in GLV10 treated roots may be unable to undergo asymmetric cell divisions until they have expanded sufficiently, impairing lateral organ initiation (Jones et al., 2019).

Impact of GOLVEN10 on transcript-level regulation of cell division and expansion

The observed phenotype in GLV10-treated root cells – increased number of cells that failed to expand (Figure 7; Figure S11), led us to propose two hypotheses regarding the underlying molecular mechanisms. Within the transcriptomic dataset described herein (Figure 8a; Table S3), we noted a downregulation of several genes essential for microtubule movement and assembly. This encompassed three *TPX2* and *TPXL5* genes (Medtr4g078565, Medtr7g013070, Medtr6g015010) essential for mitotic spindle assembly. Mutations in Arabidopsis *tpxl-5* results in a phenotypic alteration characterized by a reduced number of lateral roots, delayed lateral root initiation and wider cells as is seen upon GOLVEN treatment or overexpression (Qian et al., 2023). Proper microtubule assembly is, therefore, required for spindle formation, which is central to accurate chromosome segregation during cell division leading to cells that either divide prematurely or improperly, potentially leading to the shorter cell phenotype observed (Figure 7) (Qian et al., 2023; Wasteneys & Ambrose, 2009). The TPX2 and TPXL2 proteins facilitate interactions with spindle microtubules through their associations AURORA kinases and Kinesins. In Medicago, *AUR1* (Medtr3g110405) is expressed throughout the nodule (Gao et al., 2022). When *aur1* was downregulated using tissue specific gene editing, there was a marked decrease in the initiation of nodule primordia. This observation aligns with the reduced nodule initiation seen in plants treated with GLV10, which inhibits *MtAUR1* expression (Figures 5 and 8). Of the ten downregulated Kinesins we identified, orthologs of the functionally characterized AtKINESIN12-E (Medtr2g087840) that has a role in spindle assembly within the phragmoplast during cell division (Herrmann et al., 2021). The *kinesin12e* mutants have shorter spindles that are delayed in their formation. Kinesins are microtubule-based motor proteins essential for the proper formation of the spindle apparatus, phragmoplast, and the preprophase band during cell division. If their function is compromised, it could lead to inefficient chromosome segregation, potentially explaining the cell division abnormalities in GLV10-treated roots.

Secondly, while our data uncovered several regulators of different hormone pathways which may be expected given that optimal plant growth is a result of coordination between several hormone signaling pathways; we found a 30% overlap between genes that were regulated both by

auxin and GLV10 suggesting the peptide brings about its effects by modulating the auxin pathway (Figure S12, Table S5). Auxin plays a significant role in cell division, differentiation, and expansion by ensuring proper gradients along the root (Leyser, 2018). Our data indicate that GLVs inhibit organ formation by disrupting auxin gradients downstream of NIN, which is required for localized auxin maxima formed at nodule primordia crucial for organogenesis (Schiessl et al., 2019). GLVs do so by inducing genes encoding auxin efflux transporters (PILS2, PINs), and deregulating auxin signaling (Table S3, Figure S12). Given that expression of GLVs is modulated by Auxin (Figure 2b), it indicates that there exists a feedback mechanism that ensures timely and spatially appropriate nodule organogenesis.

The repression of genes responsible for spindle assembly and cell cycle progression suggests that GLV10 impacts both the division and subsequent expansion of cells. The intricate machinery governing plant cell division and expansion has long been a focal point of root biology research, and our findings shed light on a key player in this process, GLV10.

Unanswered questions and future prospects

A question that remains unanswered is whether the nodulation zone is identical to the rhizobial infection susceptible zone given that nodule organogenesis and rhizobial infection are genetically separable processes. The finding that GLV10 application reduces nodule density over the total root length without changing infection thread density (Figure S4), combined with the observation that none of the five GLVs are expressed *in vivo* within infected root hairs (Figure 2; Figure S4) suggests that GLV10 controls cortical processes that regulate organogenesis rather than infection. Nevertheless, since the rhizobial susceptibility zone is narrower compared to the primary root length, further studies are required to understand GLV control of rhizobial infection including changes in root hair length, root hair density and length of the susceptibility zone upon GLV10 application.

CONCLUSION

In conclusion, our study introduces a family of peptide-coding genes, namely the GOLVEN signaling peptides, into the story of root nodule symbiosis. We looked at how GLVs help legumes initiate and arrange their nodules on the primary acting downstream of the central regulator of symbiosis – NIN. We introduced the idea of 'noduletaxis'—how plants decide where to place nodules. The precise spatial placement of nodules and lateral roots, respectively, offers new perspective on how plants maintain organ number to optimize nitrogen acquisition. These data may suggest that the combined action of GLVs and auxin might have been crucial for plants as they evolved to grow on land. GLVs, found in land plants but not in rootless chlorophytes, may help plants adapt their roots based on nutrient stress signals. Although, a lot remains to be discovered, our work presented here sets the stage for future work on this interesting new family of nodulation regulators.

MATERIALS AND METHODS

Plant material, nodulation assays and growth conditions

Medicago truncatula ecotype Jemalong A17 or R108 were used in this study. All *Tnt1* mutants are in the R108 background. *Tnt1* lines isolated include *glv10-1* (NF12742), and *glv10-2* (NF20983). Seeds were scarified with concentrated H_2SO_4, and surface sterilized with undiluted household bleach (Clorox, Oakland, CA, USA) at 8% sodium hypochlorite and sown on 1% water agarose (Life Technologies Catalog: 16500100, Carlsbad, CA, USA) plates.

Seeds were stratified at 4°C for 3 days in dark prior to overnight germination at 24°C and then transferred onto agarose plates containing B&D nutrients (Broughton & Dilworth, 1971) plus 0.5 mM KNO_3 with and without peptides. Eight to ten seedlings per line were placed on each plate between sterile filter paper sheets for all experiments except the GWAS screen in which we placed three seedlings per plate. For experiments in soil, overnight germinated seedlings were transferred to a 2:1 mixture of turface:vermiculite. Plants were watered B&D solution containing six millimolar nitrogen before inoculation with rhizobia at 7 days post germination. Post Inoculation, plants were subsequently watering with B&D nutrient media supplemented with 0.5 mM Potassium Nitrate. All experiments were conducted in a controlled environment chamber at 24°C under 16 h light, 8 h dark conditions.

Arabidopsis thaliana wild type Col-0 or mutant lines were sterilized using bleach and 70% ethanol. After stratification for 3 days at 4°C, seeds were placed onto ½ MS (Murashige & Skoog) media plates with or without peptide and allowed to grow for 14 days. All plants were scored on the same day under a 4x Leica S7 microscope.

Cloning of promoters and CDS for hairy root

Gene coding regions were cloned either using Golden gate technology or the Gibson assembly method. Promoter regions of *MtGLV1* (1392 bps), *MtGLV2* (2883 bps), *MtGLV6* (2131 bps), *MtGLV9* (2192 bps), were cloned upstream of the β-Galactouronidase (GUS) gene in MU06 vector carrying a DsRed selection cassette using Gibson assembly method (Gibson et al., 2009). The *MtGLV10* endogenous promoter was synthesized (3000 bps) and cloned upstream of the GUS gene using Golden Gate cloning. All clones were verified by sanger sequencing before transformation into *M. truncatula* hairy roots mediated by *Agrobacterium rhizogenes* Arqua1 (Quandt et al., 1993). All cloned CDS using golden gate cloning (MtGLV1, MtGLV9, MtGLV10) and Gibson cloning (MtGLV2, MtGLV6) were cloned downstream of the Lotus *UBIQUITIN* promoter. Sequenced clones are available from Addgene under the deposit ID 79021.

Hairy root transformation

A streptomycin resistant strain of *A. rhizogenes* Arqua1 was transformed with constructs of interest carrying a *AtUBI:dsred* selection marker and cultured on LB medium agar plates supplemented with the corresponding antibiotics for 2 days at 28°C, Agrobacteria

were scraped off the plates using sterile spreaders and resuspended using 500–700 μl of sterile water. Root tips from overnight germinated seedlings were cut off to ensure that the meristem was completely removed and the cut end dipped in aforementioned bacterial suspension. Seedlings were transferred to and grown on modified Fahraeus medium plates for 2 weeks at 24°C 16 h day and 8 h night conditions. Transgenic calli expressing dsRed were selected using an Olympus SZX microscope and transferred to soil.

Histochemical localization of GUS and β-Gal staining

For X-gluc staining, X-GlcA ((5-bromo-4-chloro-3-indolyl-beta-D-glucuronic acid, Goldbio) in DMF (Dimethyl formamide)) was added to 50 ml of phosphate buffer (100 mM phosphate buffer saline with 100 mM Na_2HPO_4, NaH_2PO_4 each) and 50 mM K_4FeCN_6 and K_3FeCN_6 each, 0.5 M EDTA and 10% Triton X-100. X-gluc was added to a final concentration of 100 mg/100 ml buffer. Harvested root tissue were vacuum infiltrated with the X-Gluc solution for 10 min and then incubated at 37°C in dark for varying time periods. Two distinct GUS staining times were used for each construct at early nodulation time points (4 dpi, 10 dpi) and 28 dpi. These were *MtGLV1* (2, 2 h), *MtGLV2* (24, 24 h), *MtGLV6* (24 , 12 h), *MtGLV9* (4, 4 h), *MtGLV10* (24, 4 h), *MtD14* (6, 6 h), *MtSPL5* (6, 24 h) and *MtMAKRL* (24, 6 h). At 28 dpi, nodules were excised and cleared with 1/20 strength bleach overnight and imaged.

Samples were washed in phosphate buffer three times before staining rhizobia with X-gal (Goldbio). Prior to X-gal (5-bromo-4-chloro-3-indolyl-β-D-galactopyranoside) staining, tissue was fixed in 2.5% glutaraldehyde by vacuum infiltration for 10 min followed by a one-hour incubation time. Samples were rinsed with Z-buffer (100 mM Na2HPO4 and NaH2PO4 each, 10 mM Potassium chloride and 1 mM Magnesium chloride) and immediately transferred to the X-gal solution in Z-buffer (50 mM each K4FeCN6 and K3FeCN6, 4% X-gal in DMF). Tissue was vacuum infiltrated, incubated in the dark overnight and imaged the next day.

Hormone treatments and nodule excision

Peptides synthesis was carried out by Pepscan and Austin Chemicals, Inc. For auxin treatments, overnight germinated *M. truncatula* seedlings were transferred onto 1% water agarose media and grown for 3 days at 24°C. Sixty to seventy seedlings were transferred to sterile water (pH adjusted to 6.8) containing 1 uM Indole-3-acetic acid or equivalent amount of DMSO (Dimethoxy sulfoxide – solvent control) and treatment allowed to proceed for 3 h. Post treatment for 3 h, roots were excised from 20 seedlings per replicate per biological replicate and shoots discarded. For variable-N treatments, seedlings were grown for 3 days on B&D media with six mM nitrogen before transfer to liquid B&D medium at two different N-concentrations. Solution designated as Full-N constituted six mM nitrogen (Final concentration 0.5 mM KH_2PO_4, 0.25 mM K_2SO_4, 0.25 mM $MgSO_4$, 0.01 mM Fe-citrate, 1 mM $CaCl_2$, 2 mM KNO_3, 2 mM NH_4NO_3, pH 6.8) while Low-N solution contained a limited amount of nitrogen, prepared without any NH_4NO_3 and only 0.5 mM KNO_3.

RNA extraction, complimentary DNA synthesis and quantitative PCR

Total RNA was extracted using Trizol Reagent (Life Technologies) following the manufacturer's recommendations (Invitrogen GmbH, Karlsruhe, Germany), digested with RNase free DNase1 (Ambion Inc., Houston, TX) and column purified with RNeasy MinElute CleanUp Kit (Qiagen). RNA was quantified using a Nanodrop Spectrophotometer ND-100 (NanoDrop Technologies, Wilington, DE). RNA integrity was assessed on an Agilent 2100 BioAnalyser and RNA 6000 Nano Chips (Agilient Technologies, Waldbronn, Germany). First-strand complementary DNA was synthesized by priming with oligo-dT_{20} (Qiagen, Hilden, Germany), using Super Script Reverse Transcriptase III (Invitrogen GmbH, Karlsruhe, Germany) following manufacturer's recommendations. Primer Express V3.0 software was used for primer design. qPCR reactions were carried out in an QuantStudio7 (Thermo Fisher Scientific Inc, Waltham, MA, USA). Five microliters reactions were performed in an optical 384-well plate containing 2.5 μl SYBR Green Power Master Mix reagent (Applied Biosystems, Waltham, MA, USA), 15 ng cDNA and 200 nM of each gene-specific primer. Transcript levels were normalized using the geometric mean of two housekeeping genes, *MtUBI* (Medtr3g091400) and *MtPTB* (Medtr3g090960). Three biological replicates were included and displayed as relative expression values. Primer sequences are provided in Table S3.

Root embedding and sectioning

One cm root segments were fixed with 5% glutaraldehyde in Phosphate Buffer Saline (pH = 7.2) solution overnight. Samples were rinsed three times and dehydrated using ethanol gradients (20%, 40%, 60%, 80% and 100%). The samples were embedded in Technovit 7100 (Heraeus-Kulzer, Wehrheim, Germany), according to the manufacturer's protocol. Samples were sectioned to 2.5 μm thickness using a microtome and stained with Toluidine blue for 1 min or till the desired color intensity developed and rinsed three times before imaging.

Statistical analysis

All statistical analyses were performed using GraphPad Prism 8 and tests selected therein. A two-sided Student's *t*-test was used for comparison between genotypes or treatments. For multiple genotypes ordinary one-way analysis of variance tests or the Brown-Forsythe and Welch tests were performed followed by post hoc statistical tests as mentioned.

Figure preparation and R packages used

Figures were prepared using Adobe Illustrator Creative cloud. Images were edited using Adobe Photoshop and FIJI. Graphs were prepared using GraphPad Prism 8. Phylogenetic tree was prepared using Mega X and the FigTree Application. All default plots were edited using Adobe Illustrator for clarity.

Phylogenetic tree construction

Orthologs of GLV peptide encoding genes were retrieved from 18 different species by performing a Smith-Waterman search with SSearch (Ropelewski et al., 2003), and e-values of ≤0.01 were used for significant homologies followed by manual BLAST searches. Both the full protein as well as the short peptide-coding region of known peptides in Arabidopsis and Medicago were used to initiate these searches. Retrieved sequences were selected through the SSP classification pipeline on MtSSPdb.noble.org. A maximum likelihood phylogenetic tree of the resulting list of putative GLV peptide-coding proteins was generated using Mega X software and 1000 bootstrap iterations performed. Consensus tree was modified using Figtree and Adobe Illustrator.

RNA-Seq and gene expression analyses

For RNA-seq library preparation, 1 μg of total RNA was used with the TruSeq Stranded mRNA Library Prep Kit (Illumina Inc, San

Diego, CA, USA), following the kit's guidelines. Before initiating library construction, an evaluation of RNA integrity was conducted using the TapeStation 4200 (Agilent). Only samples exhibiting an RNA integrity number (RIN) exceeding nine were considered. The subsequent RNA-seq libraries underwent a size distribution check through TapeStation, followed by quantification with the Qubit 2.0 Fluorometer (Thermo Fisher Scientific). These libraries were then forwarded to Novogene Inc. for sequencing, using the Illumina Hiseq4000 (Illumina) platform with a 150 bp paired-end configuration. The anticipated depth for the sequencing reads ranged between 30 and 40×. The associated data can be accessed on NCBI with the SRA identifier PRJNA727610, covering Biosamples from SAMN19026351 to SAMN19026356.

RNA-Seq mapping and hierarchical clustering

Each sample underwent a rigorous quality control by removing low-quality bases and sequences of primers/adapters using Trimmomatic v0.361. Short reads (below 30 bases post-trimming) and their corresponding mate pairs were discarded. The trimmed sequences were then aligned to a re-annotated version of the *M. truncatula* genome (release 4.0_reanno) using HISAT2 v2.0.5 and default settings, employing 24 threads. Transcript assembly and quantification took place with Stringtie 1.2.4, using standard assembly parameters. A comparison of transcripts found in control and GLV treated samples was done, and alignment with the reference gene annotations was facilitated by Stringtie's "merge" function. DESeq2 was utilized for the analysis of differential gene expression. Expression fold differences were determined from average FPKM values, and genes with differential expression were identified using a *P-value* threshold of 0.05.

Differential gene expression analysis

Criteria for identifying differentially expressed genes (DEGs) included a fold change of 1.5 (log2 fold change > |0.58|) and a *P*-value of less than 0.05. To pinpoint common DEGs, analyses and comparisons between AtCEP1, MtCEP1D1, and MtCEP1D2 were facilitated using Venny 2.1.0. Further analysis involved the enrichment of Gene Ontology (GO) terms, conducted on the Legume IP V3 web platform (Dai et al., 2020). The enrichment tool on this platform derives GO terms from functional protein descriptions in UniProt and InterproScan databases. A significant GO term was determined by an adjusted *P*-value of less than 0.05. The most enriched GO terms were visualized for significant DEGs. Notable changes in nitrate, phosphate, and sulfate transporter expressions were visualized in a heatmap with specific criteria (log2FC > |0.58|), *P*-value <0.05. DEGs that were prominently upregulated, including kinases and transcription factors, were displayed in a heatmap (log2FC >2.0, indicating a fourfold change in expression), with a *P*-value <0.05. Visualization tools included GraphPad Prism 9.0.0, and post-processing was executed using Adobe Illustrator.

ACKNOWLEDGEMENTS

Authors gratefully acknowledge the help of Lynne Jacobs in the greenhouse, Lloyd Noble summer scholar Miss Sarah Dysinger for data entry and assistance with plant growth. We thank Dr. Julia Frugoli for the gift of the *sunn* mutant seeds and Dr. Yoshikatsu Matsubayashi for the gift of *rgfr1,2,3* mutant seeds. This research was funded by the award National Science Foundation Award #1444549 to Wolf Schieble and Michael Udvardi and by the United States Department of Agriculture grants 2022-38821-37353 and National Science Foundation Award #2217830 to Sonali Roy. All authors declare that they have no conflict of interest. Open access publishing facilitated by The University of Queensland, as part of the Wiley - The University of Queensland agreement via the Council of Australian University Librarians.

AUTHOR CONTRIBUTIONS

SR, ITJ, SZ, WL, KS, HKL, CB, DJ performed experiments and helped acquire and analyze data, SR interpreted data, SR, WRS, MU conceptualized this study, PXZ, GEDO, JDM, WRS, MU supervised the research, SR, MU wrote the manuscript.

SUPPORTING INFORMATION

Additional Supporting Information may be found in the online version of this article.

Figure S1. Phylogenetic analyses of GOLVEN peptide presence and distribution in different plant species. (a) Phylogenetic tree generated with PhytoT V2.0 and iTOL webtools to depict interrelations between plant species. Taxa encoding GOLVEN peptides are indicated on the right with a green check mark. Their absence is marked with a red cross. The ability to make nodules (Nod+/−), associate with mycorrhizal fungi (Myc+/−) or form roots or rhizoids (Root/Rhizoid+) is indicated by boxes of different colors. (b) Maximum likelihood tree showing interrelationship between Arabidopsis thaliana and *Medicago truncatula* GOLVEN proteins. Tree branch supports depicts outcome of 1000 bootstrap iterations. (c) Soybean Expression Atlas (https://soyatlas.venanciogroup.uenf.br/) output showing expression of GmGLV1 orthologs is restricted to nodules.

Figure S2. Expression of GLVs during nodulation, N-deprivation and in infected root hairs. Expression of GOLVEN peptide encoding genes in Medicago. (a) Quantitative-PCR estimation of GLV transcript abundance at the denoted timepoints. $*P < 0.05$, $***P < 0.001$ based on an ANOVA-protected Dunnett's multiple comparison test (vs 0 dpi uninfected roots). Error bars indicate SEM and three biological replicates per time point were used. (b) qPCR estimation of GLV transcript abundance in *M. truncatula* A17 plants deprived of Nitrogen for 2 weeks compared to plants supplemented with potassium nitrate as in de Bang et al., 20178. Student's *t*-test $*P < 0.05$. Error bars indicate SEM and three biological replicates per treatment were used. (c) GLV promoter-GUS reporter activity is absent in infection threads of *M. truncatula* hairy roots transformed with the indicated constructs four dpi with Rm1021. Rhizobia are co-stained in magenta-gal. Scale bars represent 100 μm.

Figure S3. Expression of Arabidopsis GOLVEN/ROOT MERISTEM GROWTH FACTORS under varying Nitrogen availabilities. Data were taken from Arabidopsis Root eFP browser and represent the study by Gifford et al., 2008. (a) Expression of AtGLV6 was induced in roots starved of nitrate compared to roots provided with 5 mM Nitrate in lateral root cap cells. (b) Heatmap showing expression of Arabidopsis GLV genes based on Gifford et al., 2008. Missing microarray data are indicated by crossed out cells.

Figure S4. Sequence and physiological effects of synthetic GLV peptides used in this study. (a) Logo showing conserved residues in Medicago peptides. (b) Sequence of GLV peptides synthesized in this study. (c) *M. truncatula* root images showing stages of lateral root or nodules scored in this study. Scale bars denote 500 μm. See Table S1 for trait definitions. (d) Time plots over 60 h showing effects of synthetic peptides used in this study on growth of Rm2011 dsRED in the presence of the peptides as indicated. Asterisk * indicates a significant difference for GLV6_hyp10 which was not reproducible in subsequent experiments. (e) Change in

total root length in *M. truncatula* Jemalong A17 seedling roots upon peptide treatment compared to control (no peptide). Asterisks represent $*P < 0.05$ using a post hoc Dunnett's multiple comparison test following a one-way ANOVA. (f) Change in total rhizobial infections upon peptide treatment compared to control in the same experiment. Asterisks represent $**P < 0.01$, $**P < 0.001$ using a post hoc Dunnett's multiple comparison test following a one-way ANOVA. (g)Number of infection events per cm total root in the same experiment as (e,f) above. Asterisks represent $**P < 0.01$, $**P < 0.001$ using a ANOVA-protected Dunnett's multiple comparison test. (h) Images showing infection structures in *M. truncatula* seedlings infected with Rm2011 HemA::LacZ 7 days post inoculation. Scale bars represent 100 μm.

Figure S5. Characterization of lines used in this study. Expression of individual MtGLV genes in their corresponding over expression lines. (a) *MtGLV1* (b) *MtGLV2* (c) *MtGLV6* (d) *MtGLV9* (e) *MtGLV10*. Data represent qPCR estimation of transcript abundance using hairy root tissues. Error bars indicated SEM, $n = 2$–4 per line. Student's *t*-test $*P < 0.05$, $***P < 0.001$. (f) Gene structure showing position of Tnt1 insertions in exonic regions of *glv10* mutant lines used in this study. (g) Agarose gel images showing PCR amplicons in WT R108 compared to mutants.

Figure S6. Effect of GLV10 peptide application on *M. truncatula* root growth. (a) Overview of peptide treatment and plant growth setup used in this study. (b, c) Representative images comparing effects of GLV10 peptide application to roots at 1 μM concentration compared to untreated roots. Images were taken 10 days post transfer to plates containing 1% Agarose in water.

Figure S7. Interaction of GLV10 signaling pathway with the Autoregulation of Nodulation pathway. Effect of 1 uM GLV10 peptide application on *sunn* mutant plants compared to WT R108. (a) Root length (b) Number of lateral roots on the primary root (c) Density of LRs on primary root (d) Number of nodules (e) Relative position of the first formed nodule (f) Nodulation zone. Number of plants analyzed were $n = 15, 15, 9, 10, 15, 20$. A one-way ANOVA protected by a Sidak's multiple comparison test between treated and untreated plants in each genotype was performed. Asterisks indicate $*P < 0.05$, $**P < 0.01$, $***P < 0.001$, n.s indicates not significant. (h) Heatmap showing gene expression of known components of the AON pathway as FPKM values. X represents treatments where no expression was detected. Data are average of three replicates. Student's *t*-test $***P < 0.001$. *RDN* (ROOT DETERMINED NODULATION), *CLE* (CLAVATA3/EMBRYO-SURROUNDING REGION (CLE) family), *SUNN* (SUPERNUMERIC NODULES), *CRN* (CORYNE), *TML* (TOO MUCH LOVE), *CEP* (C-terminally encoded peptide), *CRA2* (COMPACT ROOT ARCHITECTURE), *CRE1* (CYTOKININ RECEPTOR), *SKL* (SICKLE).

Figure S8. Peptide dilution curve. (a) Representative root scans showing seedling morphology 13 days post growth on B & D low-N media containing GLV10p, a modified non-sulfated version of the same peptide (nsGLV10p) and a scrambled version of the peptide (scrlGLV10p) at the concentrations indicated. See Figure S3 for sequence details. (b) Number of nodules, position of developmentally first formed nodule relative to primary root length and the resulting nodule formation zone 10 days post inoculation with *S. meliloti* strain Rm2011 dsRed at the concentrations of peptides indicated. (c) Density of lateral roots formed, position of developmentally first formed lateral root relative to primary root length and the resulting LR formation zone in the same experiment.

Figure S9. Response of the Arabidopsis thaliana *rgfr123* mutants to synthetic AtGLV10 peptide. Effect of 1 uM AtGLV10 peptide (D(sY)PKPSTRP(Hyp)RHN) application on *rgfr123* mutant plants compared to WT. (a) Root length (b) Number of lateral roots on the primary root (c) Lateral root zone (d) Absolute position of the first formed lateral root (e) absolute position of the young lateral root (f) Relative position of the first formed lateral root. Number of plants analyzed were $n = 15, 15, 25, 20$. A one-way ANOVA-protected Sidak's multiple comparison test between treated and untreated plants in each genotype was performed. Asterisks indicate $*P < 0.05$, $**P < 0.01$, $***P < 0.001$, n.s indicates not significant.

Figure S10. Characterization of *glv10* mutant plants growth responses compared to WT. (a) Root length (b) Number of lateral roots on the primary root (c) Lateral root density (d) Relative position of the first formed lateral root (e) total number of nodules (f) Number of lateral roots per cm root. (g) Relative position of the first formed nodule. Number of plants analyzed were $n = 57, 31, 33$. A one-way ANOVA-protected Dunnett's multiple comparison test between treated and untreated plants in each genotype was performed. Asterisks indicate $*P < 0.05$, $**P < 0.01$, $***P < 0.001$, n.s indicates not significant.

Figure S11. The synthetic peptide GLV10 affects cell number and cell size in Medicago roots. Images show 2.5 μm thick sections of root segments collected 4 cm below root tip at a 20× magnification. Control roots treated with solvent (a) and roots treated with 1 μM GLV10 peptide (b) for 7 days. Scale bars represent 50 μm. Segments from at least eight roots per sample were analyzed. Quantification of data shown in (a,b) using ImageJ. Application of GLV10 peptide increases root length by increasing cell number (c) but decreasing cell size in each cortical cell file (d). Roots were treated with peptide for 7 days on plates and compared to untreated roots. Student's *t*-test $***P < 0.001$. Average values are shown on the shoulder of each box plot.

Figure S12. The GOLVEN10 peptide affects the auxin signaling pathway. Comparing the transcriptomic signature of the peptide GOLVEN10 and the auxin Indole-3-acetic acid revealed a shared set of genes that were (a) Induced by both (b) Repressed by both (c) Induced by GLV10 but repressed by IAA. Data on IAA treated seedlings taken from Mtsspdb.zhaolab.org. The probability value for finding the number of shared genes between both hormones across all four comparisons is $P < 0.001$ using a hypergeometric probability test. (d) Repressed by GLV10 but induced by IAA. (e) qPCR validation of several auxin marker genes belonging to the *Aux/IAA*, *ARF*, *SAUR* and *GH3* gene families that were induced upon application of the synthetic peptide GLV10. Data are average of three biological replicates. Expression was normalized using two housekeeping genes *UBIQUITIN* and *PTB*. Student's *t*-test $*P < 0.05$, $**P < 0.01$, $***P < 0.001$.

Table S1. List of orthologous GOLVEN peptide-coding genes found across 21 plant species.

Table S2. List of Primers, constructs, and lines used in this study.

Table S3. List of Differentially expressed genes regulated by GOLVEN10 and 3-IAA application.

Table S4. Gene Ontology (GO) Enrichment Analysis Results.

Table S5. Expression Profiles of Auxin-Regulated Genes Following GLV10 Application.

OPEN RESEARCH BADGES

This article has earned an Open Data badge for making publicly available the digitally-shareable data necessary to reproduce the reported results. The data is available at the associated data can be accessed on NCBI with the SRA identifier PRJNA727610, covering Biosamples from SAMN19026351 to SAMN19026356. Overexpression constructs can be requested from Addgene – deposit ID 79021.

DATA AVAILABILITY STATEMENT

All peptide gene overexpression constructs have been deposited with Addgene and can be accessed under deposit ID 79021.

REFERENCES

Beemster, G.T. & **Baskin, T.I.** (1998) Analysis of cell division and elongation underlying the developmental acceleration of root growth in *Arabidopsis thaliana*. *Plant Physiology*, **116**, 1515–1526.

Boschiero, C., **Dai, X.**, **Lundquist, P.K.**, **Roy, S.**, **Christian De Bang, T.**, **Zhang, S.** ***et al.*** (2020) MtSSPdb: the *Medicago truncatula* small secreted peptide database. *Plant Physiology*, **183**, 399–413.

Broughton, W.J. & **Dilworth, M.J.** (1971) Control of leghaemoglobin synthesis in snake beans. *The Biochemical Journal*, **125**, 1075–1080.

Cederholm, H.M. & **Benfey, P.N.** (2015) Distinct sensitivities to phosphate deprivation suggest that RGF peptides play disparate roles in *Arabidopsis thaliana* root development. *New Phytologist*, **207**, 683–691.

Corcilius, L., **Hastwell, A.H.**, **Zhang, M.**, **Williams, J.**, **Mackay, J.P.**, **Gresshoff, P.M.** ***et al.*** (2017) Arabinosylation modulates the growth-regulating activity of the peptide hormone CLE40a from soybean. *Cell Chemical Biology*, **24**, 1347–1355.e7.

Dai, X., **Zhuang, Z.**, **Boschiero, C.**, **Dong, Y.** & **Zhao, P.X.** (2020) LegumeIP V3: from models to crops—an integrative gene discovery platform for translational genomics in legumes. *Nucleic Acids Research*, **49**, D1472–D1479.

De Bang, T.C., **Lundquist, P.K.**, **Dai, X.**, **Boschiero, C.**, **Zhuang, Z.**, **Pant, P.** ***et al.*** (2017) Genome-wide identification of Medicago peptides involved in macronutrient responses and nodulation. *Plant Physiology*, **175**, 1669–1689.

Du, Y. & **Scheres, B.** (2018) Lateral root formation and the multiple roles of auxin. *Journal of Experimental Botany*, **69**, 155–167.

Dubrovsky, J., **Gambetta, G.**, **Hernández-Barrera, A.**, **Shishkova, S.** & **González, I.** (2006) Lateral root initiation in Arabidopsis: developmental window, spatial patterning, density and predictability. *Annals of Botany*, **97**, 903–915.

Fang, T., **Motte, H.**, **Parizot, B.** & **Beeckman, T.** (2021) Early "rootprints" of plant terrestrialization: Selaginella root development sheds light on root evolution in vascular plants. *Frontiers in Plant Science*, **12**, 735514.

Fernandez, A., **Drozdzecki, A.**, **Hoogewijs, K.**, **Vassileva, V.**, **Madder, A.**, **Beeckman, T.** ***et al.*** (2015) The GLV6/RGF8/CLEL2 peptide regulates early pericycle divisions during lateral root initiation. *Journal of Experimental Botany*, **66**, 5245–5256.

Fernandez, A.I., **Vangheluwe, N.**, **Xu, K.**, **Jourquin, J.**, **Claus, L.A.N.**, **Morales-Herrera, S.** ***et al.*** (2020) GOLVEN peptide signalling through RGI receptors and MPK6 restricts asymmetric cell division during lateral root initiation. *Nature Plants*, **6**, 533–543.

Furumizu, C., **Krabberød, A.K.**, **Hammerstad, M.**, **Alling, R.M.**, **Wildhagen, M.**, **Sawa, S.** ***et al.*** (2021) The sequenced genomes of nonflowering land plants reveal the innovative evolutionary history of peptide signaling. *The Plant Cell*, **33**, 2915–2934.

Gao, J.-P., **Jiang, S.**, **Su, Y.**, **Xu, P.**, **Wang, J.**, **Liang, W.** ***et al.*** (2022) Intracellular infection by symbiotic bacteria requires the mitotic kinase AURORA1. *Proceedings of the National Academy of Sciences*, **119**, e2202606119.

Gibson, D.G., **Young, L.**, **Chuang, R.Y.**, **Venter, J.C.**, **Hutchison, C.A., III** & **Smith, H.O.** (2009) Enzymatic assembly of DNA molecules up to several hundred kilobases. *Nature Methods*, **6**, 343–345.

Goto, H., **Okuda, S.**, **Mizukami, A.**, **Mori, H.**, **Sasaki, N.**, **Kurihara, D.** ***et al.*** (2011) Chemical visualization of an attractant peptide, LURE. *Plant and Cell Physiology*, **52**, 49–58.

Herrmann, A., **Livanos, P.**, **Zimmermann, S.**, **Berendzen, K.**, **Rohr, L.**, **Lipka, E.** ***et al.*** (2021) KINESIN-12E regulates metaphase spindle flux and helps control spindle size in *Arabidopsis*. *The Plant Cell*, **33**, 27–43.

Hofhuis, H., **Laskowski, M.**, **Du, Y.**, **Prasad, K.**, **Grigg, S.**, **Pinon, V.** ***et al.*** (2013) Phyllotaxis and rhizotaxis in *Arabidopsis* are modified by three PLETHORA transcription factors. *Current Biology*, **23**, 956–962.

Huo, X., **Schnabel, E.**, **Hughes, K.** & **Frugoli, J.** (2006) RNAi phenotypes and the localization of a protein:: GUS fusion imply a role for *Medicago truncatula* PIN genes in nodulation. *Journal of Plant Growth Regulation*, **25**, 156–165.

Imin, N., **Mohd-Radzman, N.A.**, **Ogilvie, H.A.** & **Djordjevic, M.A.** (2013) The peptide-encoding CEP1 gene modulates lateral root and nodule numbers in *Medicago truncatula*. *Journal of Experimental Botany*, **64**, 5395–5409.

Isidra-Arellano, M.C., **Pozas-Rodríguez, E.A.**, **Del Rocío Reyero-Saavedra, M.**, **Arroyo-Canales, J.**, **Ferrer-Orgaz, S.**, **Del Socorro Sánchez-Correa, M.** ***et al.*** (2020) Inhibition of legume nodulation by pi deficiency is dependent on the autoregulation of nodulation (AON) pathway. *The Plant Journal*, **103**, 1125–1139.

Jones, A.R., **Band, L.R.** & **Murray, J.A.** (2019) Double or nothing? Cell division and cell size control. *Trends in Plant Science*, **24**, 1083–1093.

Jourquin, J., **Fernandez, A.I.**, **Xu, K.**, **Simura, J.**, **Ljung, K.** & **Beeckman, T.** (2022) GOLVEN peptides regulate lateral root spacing as part of a negative feedback loop on the establishment of auxin maxima. *bioRxiv*, 2022.09. 26.509595.

Laffont, C., **Ivanovici, A.**, **Gautrat, P.**, **Brault, M.**, **Djordjevic, M.A.** & **Frugier, F.** (2020) The NIN transcription factor coordinates CEP and CLE signaling peptides that regulate nodulation antagonistically. *Nature Communications*, **11**, 3167.

Laporte, P., **Lepage, A.**, **Fournier, J.**, **Catrice, O.**, **Moreau, S.**, **Jardinaud, M.-F.** ***et al.*** (2014) The CCAAT box-binding transcription factor NF-YA1 controls rhizobial infection. *Journal of Experimental Botany*, **65**, 481–494.

Laskowski, M. & **Ten Tusscher, K.H.** (2017) Periodic lateral root priming: what makes it tick? *The Plant Cell*, **29**, 432–444.

Leyser, O. (2018) Auxin signaling. *Plant Physiology*, **176**, 465–479.

Li, Q., **Li, M.**, **Zhang, D.**, **Yu, L.**, **Yan, J.** & **Luo, L.** (2020) The peptide-encoding *MtRGF3* gene negatively regulates nodulation of *Medicago truncatula*. *Biochemical and Biophysical Research Communications*, **523**, 66–71.

Li, Q., **Shan, D.**, **Zheng, W.**, **Wang, Y.**, **Lin, Z.**, **Jin, H.** ***et al.*** (2023) MtRGF3 peptide activates defense responses and represses the expressions of nodulation signaling genes in *Medicago truncatula*: activation of defense response by MtRGF3p. *Acta Biochimica et Biophysica Sinica*, **55**, 1319.

Lynch, J.P. (2019) Root phenotypes for improved nutrient capture: an underexploited opportunity for global agriculture. *New Phytologist*, **223**, 548–564.

Maekawa, T., **Kusakabe, M.**, **Shimoda, Y.**, **Sato, S.**, **Tabata, S.**, **Murooka, Y.** ***et al.*** (2008) Polyubiquitin promoter-based binary vectors for overexpression and gene silencing in *Lotus japonicus*. *Molecular Plant-Microbe Interactions*, **21**, 375–382.

Matsuzaki, Y., **Ogawa-Ohnishi, M.**, **Mori, A.** & **Matsubayashi, Y.** (2010) Secreted peptide signals required for maintenance of root stem cell niche in *Arabidopsis*. *Science*, **329**, 1065–1067.

Meng, L., **Buchanan, B.B.**, **Feldman, L.J.** & **Luan, S.** (2012) CLE-like (CLEL) peptides control the pattern of root growth and lateral root development in *Arabidopsis*. *Proceedings of the National Academy of Sciences*, **109**, 1760–1765.

Mens, C., **Hastwell, A.H.**, **Su, H.**, **Gresshoff, P.M.**, **Mathesius, U.** & **Ferguson, B.J.** (2021) Characterisation of *Medicago truncatula* CLE34 and CLE35 in nitrate and rhizobia regulation of nodulation. *New Phytologist*, **229**, 2525–2534.

Michniewicz, M., **Ho, C.-H.**, **Enders, T.A.**, **Floro, E.**, **Damodaran, S.**, **Gunther, L.K.** ***et al.*** (2019) TRANSPORTER OF IBA1 links auxin and cytokinin to influence root architecture. *Developmental Cell*, **50**, 599–609.e4.

Mohd-Radzman, N.A., **Djordjevic, M.A.** & **Imin, N.** (2013) Nitrogen modulation of legume root architecture signaling pathways involves phytohormones and small regulatory molecules. *Frontiers in Plant Science*, **4**, 385.

Mohd-Radzman, N.A., **Laffont, C.**, **Ivanovici, A.**, **Patel, N.**, **Reid, D.**, **Stougaard, J.** ***et al.*** (2016) Different pathways act downstream of the CEP peptide receptor CRA2 to regulate lateral root and nodule development. *Plant Physiology*, **171**, 2536–2548.

Moreau, C., **Gautrat, P.** & **Frugier, F.** (2021) Nitrate-induced CLE35 signaling peptides inhibit nodulation through the SUNN receptor and miR2111 repression. *Plant Physiology*, **185**, 1216–1228.

Mortier, V., **Den Herder, G.**, **Whitford, R.**, **Van De Velde, W.**, **Rombauts, S.**, **D'haeseleer, K.** ***et al.*** (2010) CLE peptides control *Medicago truncatula* nodulation locally and systemically. *Plant Physiology*, **153**, 222–237.

Nishida, H., **Tanaka, S.**, **Handa, Y.**, **Ito, M.**, **Sakamoto, Y.**, **Matsunaga, S.** ***et al.*** (2018) A NIN-LIKE PROTEIN mediates nitrate-induced control of root nodule symbiosis in *Lotus japonicus*. *Nature Communications*, **9**, 499.

Nishihama, R., **Soyano, T.**, **Ishikawa, M.**, **Araki, S.**, **Tanaka, H.**, **Asada, T.** ***et al.*** (2002) Expansion of the cell plate in plant cytokinesis requires a kinesin-like protein/MAPKKK complex. *Cell*, **109**, 87–99.

Okamoto, S., **Shinohara, H.**, **Mori, T.**, **Matsubayashi, Y.** & **Kawaguchi, M.** (2013) Root-derived CLE glycopeptides control nodulation by direct binding to HAR1 receptor kinase. *Nature Communications*, **4**, 2191.

Okuda, S., **Tsutsui, H.**, **Shiina, K.**, **Sprunck, S.**, **Takeuchi, H.**, **Yui, R.** ***et al.*** (2009) Defensin-like polypeptide LUREs are pollen tube attractants secreted from synergid cells. *Nature*, **458**, 357–361.

Okuma, N., **Soyano, T.**, **Suzaki, T.** & **Kawaguchi, M.** (2020) MIR2111-5 locus and shoot-accumulated mature miR2111 systemically enhance nodulation depending on HAR1 in *Lotus japonicus*. *Nature Communications*, **11**, 1–13.

Penmetsa, R.V. & **Cook, D.R.** (1997) A legume ethylene-insensitive mutant hyperinfected by its rhizobial symbiont. *Science*, **275**, 527–530.

Penmetsa, R.V., **Frugoli, J.A.**, **Smith, L.S.**, **Long, S.R.** & **Cook, D.R.** (2003) Dual genetic pathways controlling nodule number in *Medicago truncatula*. *Plant Physiology*, **131**, 998–1008.

Qian, Y., **Wang, X.**, **Liu, Y.**, **Wang, X.** & **Mao, T.** (2023) HY5 inhibits lateral root initiation in *Arabidopsis* through negative regulation of the microtubule-stabilizing protein TPXL5. *The Plant Cell*, **35**, 1092–1109.

Quandt, H.J., **Pühler, A.** & **Broer, I.** (1993) Transgenic root nodules of Vicia hirsuta: a fast and efficient system for the study of gene expression in indeterminate-type nodules. *MPMI-Molecular Plant Microbe Interactions*, **6**, 699–706.

Ropelewski, A.J., **Nicholas, H.B., Jr.** & **Deerfield, D.W.** (2003) Mathematically complete nucleotide and protein sequence searching using search. *Current Protocols in Bioinformatics*, **4**, 3–10.

Roy, S., **Griffiths, M.**, **Torres-Jerez, I.**, **Sanchez, B.**, **Antonelli, E.**, **Jain, D.** ***et al.*** (2022) Application of synthetic peptide CEP1 increases nutrient uptake rates along plant roots. *Frontiers in Plant Science*, **12**, 793145.

Roy, S., **Liu, W.**, **Nandety, R.S.**, **Crook, A.**, **Mysore, K.S.**, **Pislariu, C.I.** ***et al.*** (2020) Celebrating 20 years of genetic discoveries in legume nodulation and symbiotic nitrogen fixation. *The Plant Cell*, **32**, 15–41.

Roy, S. & **Muller, L.M.** (2022) A rulebook for peptide control of legume-microbe endosymbioses. *Trends in Plant Science*, **27**, 870–889.

Roy, S., **Robson, F.**, **Lilley, J.**, **Liu, C.-W.**, **Cheng, X.**, **Wen, J.** ***et al.*** (2017) MtLAX2, a functional homologue of the *Arabidopsis* auxin influx transporter AUX1, is required for nodule organogenesis. *Plant Physiology*, **174**, 326–338.

Schiessl, K., **Lilley, J.L.S.**, **Lee, T.**, **Tamvakis, I.**, **Kohlen, W.**, **Bailey, P.C.** ***et al.*** (2019) NODULE INCEPTION recruits the lateral root developmental program for symbiotic nodule organogenesis in *Medicago truncatula*. *Current Biology*, **29**, 3657–3668.e5.

Shinohara, H., **Mori, A.**, **Yasue, N.**, **Sumida, K.** & **Matsubayashi, Y.** (2016) Identification of three LRR-RKs involved in perception of root meristem growth factor in *Arabidopsis*. *Proceedings of the National Academy of Sciences*, **113**, 3897–3902.

Stegmann, M., **Zecua-Ramirez, P.**, **Ludwig, C.**, **Lee, H.S.**, **Peterson, B.**, **Nimchuk, Z.L.** ***et al.*** (2022) RGI-GOLVEN signaling promotes cell surface immune receptor abundance to regulate plant immunity. *EMBO Reports*, **23**, e53281.

Tabata, R., **Sumida, K.**, **Yoshii, T.**, **Ohyama, K.**, **Shinohara, H.** & **Matsubayashi, Y.** (2014) Perception of root-derived peptides by shoot LRR-RKs mediates systemic N-demand signaling. *Science*, **346**, 343–346.

Tadege, M., **Wen, J.**, **He, J.**, **Tu, H.**, **Kwak, Y.**, **Eschstruth, A.** ***et al.*** (2008) Large-scale insertional mutagenesis using the *Tnt1* retrotransposon in the model legume *Medicago truncatula*. *The Plant Journal*, **54**, 335–347.

Wang, C., **Yu, H.**, **Zhang, Z.**, **Yu, L.**, **Xu, X.**, **Hong, Z.** ***et al.*** (2015) Phytosulfokine is involved in positive regulation of *Lotus japonicus* nodulation. *Molecular Plant Microbe Interactions*, **28**, 847–855.

Wasteneys, G.O. & **Ambrose, J.C.** (2009) Spatial organization of plant cortical microtubules: close encounters of the 2D kind. *Trends in Cell Biology*, **19**, 62–71.

Whitford, R., **Fernandez, A.**, **Tejos, R.**, **Pérez, A.C.**, **Kleine-Vehn, J.**, **Vanneste, S.** ***et al.*** (2012) GOLVEN secretory peptides regulate auxin carrier turnover during plant gravitropic responses. *Developmental Cell*, **22**, 678–685.

Yoshida, C., **Funayama-Noguchi, S.** & **Kawaguchi, M.** (2010) Plenty, a novel hypernodulation mutant in *Lotus japonicus*. *Plant and Cell Physiology*, **51**, 1425–1435.

Zhu, F., **Deng, J.**, **Chen, H.**, **Liu, P.**, **Zheng, L.**, **Ye, Q.** ***et al.*** (2020) A CEP peptide receptor-like kinase regulates auxin biosynthesis and ethylene signaling to coordinate root growth and symbiotic nodulation in *Medicago truncatula*. *The Plant Cell*, **32**, 2855–2877.